https://doi.org/10.5194/wes-2025-41
Preprint. Discussion started: 21 March 2025

eawe european academy of wind energy
Open Access WIND ENERGY SCIENCE DISCUSSIONS

Scour variability across offshore wind farms (OWFs): Understanding site-specific scour drivers as a step towards assessing potential impacts on the marine environment

Karen Garcia[1*], Christian Jordan[1], Gregor Melling[3], Alexander Schendel[1,2], Mario Welzel[1], Torsten Schlurmann[1,2]

[1]Leibniz University Hannover, Ludwig-Franzius-Institute for Hydraulic, Estuarine and Coastal Engineering, Nienburger Str. 4, 30167 Hannover, Germany. Email: schendel@lufi.uni-hannover.de, jordan@lufi.uni-hannover.de, welzel@lufi.uni-hannover.de, schlurmann@lufi.uni-hannover.de

[2]Coastal Research Centre, Leibniz University Hannover & Technical University Braunschweig, Merkurstraße 11, 30419 Hannover, Germany.

[3] Federal Waterways Engineering and Research Institute (BAW), Wedeler Landstraße 157, 22559 Hamburg, Germany. Email: gregor.melling@baw.de

[*]Corresponding author: garcia@lufi.uni-hannover.de

Abstract: The development of offshore wind farms (OWFs) is critical to meeting renewable energy targets, but predicting scour around offshore wind energy structures (OWES) and the associated potential impacts on marine ecosystems remains a challenge. Using high-resolution bathymetry data, this study analyses field-measured scour depths at 460 monopiles at nine British OWFs. The analysis reveals a large spatial variability of relative scour depths (S/D) between OWF sites, but also within individual wind farms. Principal component analysis (PCA) is used to identify significant drivers of this variability. When the entire data set is considered, results indicate that median grain size (D_{50}), relative water depths (h/D), and the significant wave height ($H_{s,99}$) are the most important influencing factors for the variability of scour depths. Other parameters investigated, such as Froude number (Fr), pile Reynolds number (Re), flow intensity ($U_{c,99}/U_{cr}$), and current velocity ($U_{c,99}$), were found to have a less clear influence. Further sediment-specific analysis shows that relative water depth (h/D) is a particularly relevant driver of scour at sites with fine (63 to 200 μm) and medium sands (200 to 630 μm), with larger scour depths occurring in shallower water depths. Findings from this study provide new insights into scour behavior across a range of spatial and environmental scales and lay a foundation for the transferability of scour prediction frameworks to new OWF sites. In the future, findings and datasets from this study are suggested to be used to estimate scour-induced sediment transport and thereby to provide a step towards the assessment of potential impacts of OWF expansion scenarios in the marine environment. By addressing the broader implications for regional sediment dynamics, this research contributes to the sustainable development of offshore wind energy.

Keywords: Offshore wind farms (OWFs), scour depths, monopile, sediment transport, principal component analysis (PCA).

https://doi.org/10.5194/wes-2025-41
Preprint. Discussion started: 21 March 2025

eawe european academy of wind energy
Open Access WIND ENERGY SCIENCE DISCUSSIONS

1 Introduction & Motivation

The expansion of renewable energy is crucial for a sustainable and independent energy supply. In order to meet the European Union's targets for expanding offshore wind energy (EU, 2020), it is necessary to develop areas with previously unveiled metoceanic and geophysical conditions. To this end, existing knowledge gaps about the interaction of individual offshore wind energy structures (OWES) or entire offshore wind farms (OWFs) with the marine environment must be closed. In general, the disturbance of the flow by an offshore structure causes scour, which might not only affect the structure's stability (Saathoff et al., 2024), but the mobilized sediment may also contribute to the overall regional sediment transport (Vanhellemont et al. 2014; Baeye et al. and Fettweis et al., 2015; Rivier et al. 2016) with potential impacts on the marine environment.

The scour process itself, is a multivariate process, which is dependent on a combination of complex hydrodynamic and geotechnical drivers. Early studies focused on the understanding of the scour process around a pile under simplified isolated hydraulic conditions, such as steady flow (e.g., Sheppard et al., 2004; Zhao et al., 2012; Sarkar et al., 2014; Baykal et al., 2015), unsteady and bidirectional tidal currents (e.g. Escarameia and May1999; McGovern et al., 2014; Yao et al., 2016; Schendel et al, 2018) and waves (e.g. Sumer et al.,1992b; Carreiras et al., 2001; Stahlmann et al., 2013). With the availability of more sophisticated experimental facilities and numerical models, research is increasingly shifting toward more complex hydrodynamic loads consisting of a combination of waves and currents, as in the studies of Sumer and Fredsøe (2001), Qi and Gao (2014), Schendel et al (2020), Lyu et al. (2021), and Du et al. (2022) but also towards studies addressing complex offshore structures (Welzel, 2021; Welzel et al., 2024; Sarmiento et al., 2024; Chen et al. 2025).

Despite those advances in scour research, uncertainties remain in current scour prediction methods (Chen et al., 2024). Matutano et al. (2013) demonstrated the challenges of applying empirical formulas for maximum scour depths by comparing different methods with data from ten European OWFs, revealing overpredictions in all but two cases. The comparison highlights the fundamental challenge of accounting for complex marine flow conditions, characterized by the superposition of multiple influencing factors, such as flow velocity, sediment coarseness, and wave-current interactions, in the prediction of scour processes using existing models (Gazi et al., 2020; Harris eat al. 2023)

Compared to laboratory experiments focusing on scour processes, rather few studies are based on in-situ data, that represent the actual scour development under complex flow conditions. These studies assessed the scour at individual structures, such as monopiles (Walker, 1995; Noormets et al., 2003; Harris et al., 2004; Rudolph et al., 2004; Louwersheimer et al., 2009), and jackets (Bolle et al., 2012; Baelus et al., 2018; Harris and Whitehouse et al., 2021), or dealt with larger datasets from entire offshore wind projects (DECC 2008; COWRIE 2010; Whitehouse et al. 2010; Whitehouse et al., 2011; Melling (2015)), covering both spatial and temporal evolution of scour under different hydrodynamic regimes and seabed types across the North Sea and British continental shelf. In general, the amount and variety of field data collected has increased with the gradual installation of offshore wind turbines. Focusing specifically on the correlation between scour and on-site conditions, Melling (2015) analyzed the relationships between the variations of scour hole dimension within OWFs and both sedimentological and hydrodynamic parameters of 281 turbines in the Outer Thames estuary. Melling's (2015) study, although only covering three OWFs, represents one of the most comprehensive investigations of field related scour to date, with the highest number of structures examined

https://doi.org/10.5194/wes-2025-41
Preprint. Discussion started: 21 March 2025

eawe european academy of wind energy
Open Access WIND ENERGY SCIENCE DISCUSSIONS

so far. By comparing field data with physical modeling experiments and literature, the study provided valuable insights into the range of observed scour and its controlling structural hydrodynamic, and sedimentological parameters.

In addition to local scour at individual structures, the cumulative effect of multiple structures in an OWFs can alter ocean dynamics (Christiansen et al., 2022), mixing (Schultze et al., 2020) and sediment mobility (Vanhellemont & Ruddick, 2014). Increased velocities and turbulence induced by OWFs has also the potential to affect the marine environment, potentially leading to global erosion around the structures as well as habitat loss or gain for benthic flora and fauna (Shields et al., 2011; Wilson and Elliott, 2009; Welzel et al., 2019). . Concerns over the potential impacts of OWF installations on local ecosystems further include collision risks, noise pollution, electromagnetic field and the introduction of invasive species (Lloret et al., 2022; Bailey et al., 2014; Teilmann and Carstensen, 2012; Watson et al., 2024). As the size and scale of OWF increases, the risk of significant cumulative effects arising is also expected to increase (Brignon et al., 2022; Gușatu et al., 2021). The drivers and interdependencies of these large-scale processes are not yet well understood and the precise impact of scour induced sediment transport on the marine environment remains uncertain, highlighting the need for interdisciplinary research utilizing field data.

In order to gain a better understanding of the geophysical changes following the installation of OWFs and potential impacts on the marine environment arising from it, this study analyses the scour development at OWES as a first step. This study builds its analysis on field data, including high-resolution bathymetry scans from British OWFs, which have recently been made publicly available. This provides an opportunity to extend the understanding of scour evolution and its key drivers using a cross-regional dataset. A total of 460 monopiles were analyzed to obtain local scour depths and their spatial distribution in dependence of selected hydrodynamic and geological drivers.
Understanding scour development is a critical first step in assessing potential environmental impacts. It will help determine whether OWES and entire OWFs contribute to regional sediment mobilization and provide a foundation for future research into the long-term morphological footprint of OWF installations and their broader ecological effects. Towards the overall goal, the paper focuses on advancing understanding of scour at OWES by analyzing field data from 460 monopiles across 9 OWFs, situated in diverse ocean regimes with current velocities from 0.54 m/s to 1.77 m/s (99th quantile), significant wave heights from 1.5 m to 2.7 m (99th quantile), water depths from 5 to 35 m and grain sizes ranging from cohesive sediment (51.54 um) to medium gravel (19872 um). The spatial distribution and variability of scour depths across and within these OWFs are determined and correlated with selected hydrodynamic and sedimentological parameters, using Principal Component Analysis (PCA). Ultimately, the results of the study will help decrease uncertainty in scour depth prediction by assessing the contribution of the main drivers of scour development from multivariable field data.
This paper is organized as follows: Section 2 describes the study area and methodology in which the methods used to obtain the scour depths and selected on-site parameters are explained in detail (subsections 2.2 – 2.5). Additionally, the application of the Principal Component Analysis (PCA) to identify the primary correlation between these parameters and scour development is explained (subsection 2.6). The results are presented in section 3, followed by implications for scour predictions for OWF (section 4), limitations and future research (section 5) and ending with the conclusions (section 6).

https://doi.org/10.5194/wes-2025-41
Preprint. Discussion started: 21 March 2025

eawe european academy of wind energy
Open Access WIND ENERGY SCIENCE DISCUSSIONS

2 Study area and methodology

2.1 Study area

The research area, located in British waters, is illustrated in Figure 1, showing the specific locations of the nine studied OWFs. Figure 1A provides a general overview, while Figure 1B pinpoints the positions of the OWFs, labeled 1 to 9. These OWFs correspond to Robin Rigg, Barrow, Teesside, Humber Gateway, Lincs, Lynn and Inner Dowsing, Greater Gabbard, London Array, and Gunfleet Sands OWFs, respectively. Figures 1C and 1D display the 99th quantiles of the significant wave heights (H_s) and current velocity magnitudes (U_c) at the nine locations, respectively.

Notably, wind farms such as Robin Rigg and Barrow are situated in the Irish Sea, while the remaining seven are located in the North Sea at the east coast of UK (Fig 1B). Water depths (h) ranging from 5 to 35 m can be found across the nine OWFs. Depth data (h) were obtained from EMODET **(https://emodnet.ec.europa.eu/en/bathymetry)**. The OWF located in the shallowest water depths is Robin Rigg with h ranging from 1 to 14 m (Fig. 1B). Conversely, the OWF with the deepest water depths is Greater Gabbard with h ranging from 21 to 35 m (Fig. 1B).

The highest and lowest significant wave heights (99th quantile) can be found at Humber Gateway OWF (H_s= 2.7 m) (Fig. 1C-D) and at Gunfleet Sands OWF (H_s = 1.5 m), which are located at the mouths of the Humber and Thames estuaries (Fig. 1C-D), respectively. Regarding the quantile of current velocities, the highest value is found at Robin Rigg OWF with 1.8 m/s (Fig. 1C-D), while the lowest value is found at Gunfleet Sands OWF with a value of 0.4 m/s (Fig. 1C-D).

Depending on the locations of the OWFs, the seabed conditions vary from sandbanks featuring a variety of bedforms to intertidal mudflats. Accordingly, the sediment also varies from silt to coarse and very coarse gravel, with the sediment at Teeside OWF consisting of fine and silty sands and that at Humber Gateway consisting of sandy gravel and boulders. In contrast, OWFs such as London Array and Greater Gabbard are located in the Outer Thames Estuary with sandbanks and channels, while others such as Barrow and Robin Rigg have distinct geological features such as megaripples, mudflats and deposits from different geological eras.

2.2 Data description

Bathymetric datasets from the nine OWFs considered in this study were collected via multibeam echosounder (MBES) before, during and after the construction of the OWFs and were afterwards made available by its operators via the Marine Data Exchange (MDE).

In total 460 OWES (of 680 available) with monopiles foundations were analyzed in this study. For the correlation between scour and hydrodynamic conditions at the nine studied OWFs, metocean hindcast datasets (i.e., significant wave height (H_s) and velocity magnitude (U_c)) by the Copernicus Marine Service (CMEMS) (https://marine.copernicus.eu/) were used (CMEMS, 2023a, 2023b).

https://doi.org/10.5194/wes-2025-41
Preprint. Discussion started: 21 March 2025

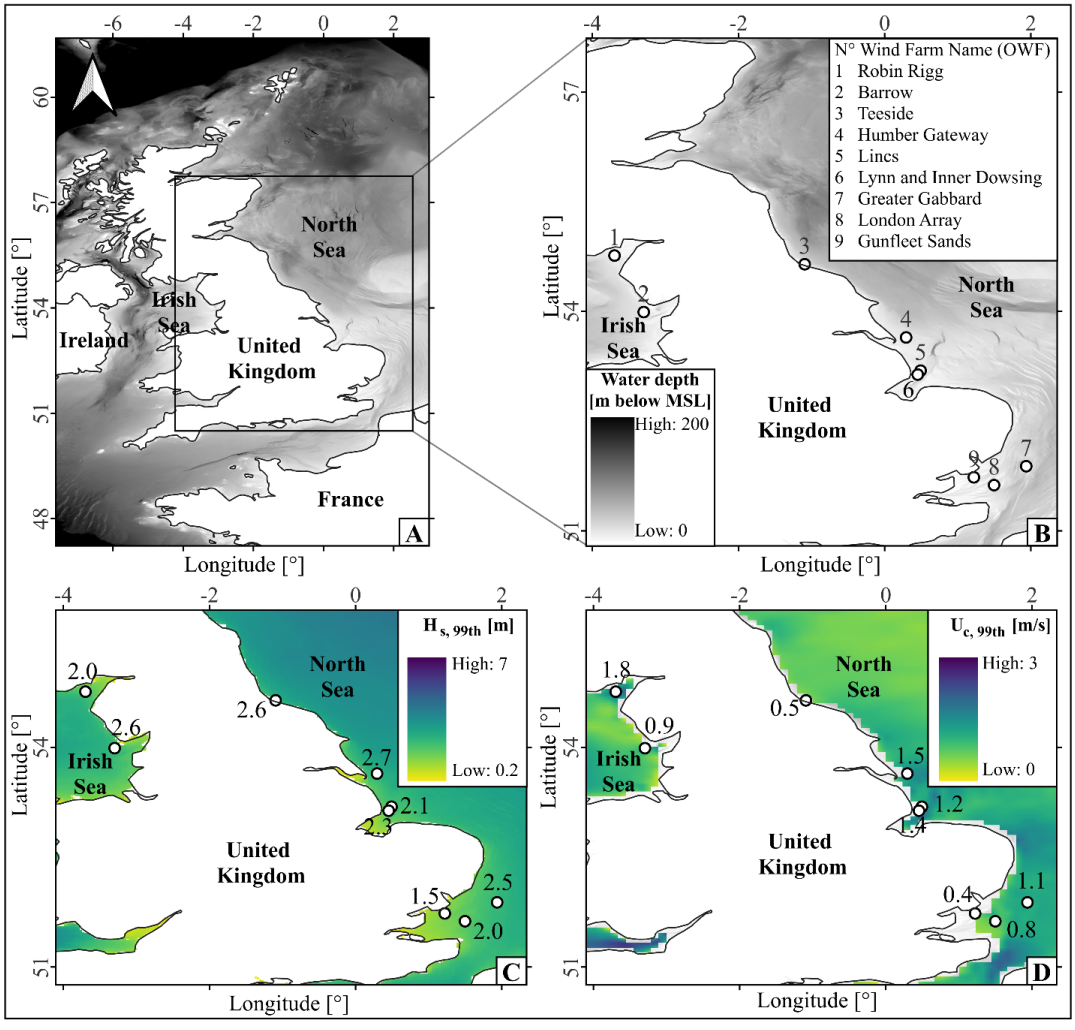

Figure 1: A) Study area. B) Location of the nine studied OWFs. Shown bathymetry data originates from EMODET (https://emodnet.ec.europa.eu/en/bathymetry). C) 99th quantile of significant wave heights (H_s) based on data for the year 2012. D) 99th quantile of current velocity magnitudes (U_c) based on data for the year 2012.

https://doi.org/10.5194/wes-2025-41
Preprint. Discussion started: 21 March 2025

eawe european academy of wind energy
Open Access WIND ENERGY SCIENCE DISCUSSIONS

Table 1 shows the OWFs considered in this study and provides an overview of their structural characteristics as well as the hydrodynamic and geotechnical site conditions. Pile diameters (D) were obtained from Negro et al. (2017), water depths (h) are based on EMODET (2020), D_{50} represents the median grain diameter of the sediment. The sediment data shown in Table 1 were obtained in Phi units from each OWF's benthic reports, then converted to D_{50} values in micrometers (μm) according to Bunte et al. (2001). The scour depth S represents the deepest scour at an individual OWES. The number of turbines varies from 26 turbines installed at Teesside OWF to 174 turbines installed at London Array OWF, indicating the different operational scales. For some OWFs, including Lynn and Inner Dowsing, extensive bathymetric data spanning over ten years was available. In contrast, others, such as Humber Gateway, had more limited bathymetric data with a coverage duration of four years. The highest grid resolutions of the bathymetric datasets found at each OWF varied from 0.2 to 0.5 m, with the highest resolution of the bathymetries found at each OWF being used. The earliest bathymetry was collected at Barrow OWF in 2005 and the most recent was collected at Lynn and Inner Dowsing in 2017, highlighting the long-term monitoring efforts at the wind farms. However, in this study only scour depths obtained from the pre- and the first post-construction bathymetries were considered. The shortest period between pre and post bathymetries was found at Lincs OWF with 377 days between August 2010 and August 2011, while the longest period between scans was detected at Greater Gabbard OWF with 2902 days (~8 yrs) between June 2005 and May 2013.

Furthermore, environmental and hydrodynamic conditions associated with each OWF are also shown in Table 1, which are essential for understanding how different variables contribute to scour around monopiles. These variables include the 99th quantile significant wave height (H_s), representing the average height of the highest third of waves. The wave height has a direct influence on the wave-induced current velocity near the seabed and thus strongly determines the bed shear stresses and the formation of the vortex system around the OWES (Sumer & Fredsøe, 2002; Schendel et al., 2018). The 99th quantile current velocity magnitude (U_c) indicates the resultant of eastward and northward tidal flow components, whereas U_{crit} depicts the critical flow velocity for sediment entrainment. Their ratio, the flow intensity (U_c/U_{cr}), is a key parameter in describing the general sediment mobility and has a large impact on the scour rate and depth (Melville and Coleman, 2000). The relative water depth (h/D) influences the formation of the horseshoe vortex in such a way that the size of the horseshoe vortex is reduced as the flow depth decreases, resulting in a reduction in the scour depth. At greater water depths ($h/D \geq 5$) the scour depth becomes almost independent of water depth (Sumer and Fredsøe, 2002).

The Froude number (Fr) and pile Reynolds number (Re) are used to characterize the flow conditions around the pile. The Froude number indicates whether the flow is dominated by gravitational or inertial forces. With increasing Froude number, pressure gradients at the pile increase, which affects the flow field in the vicinity of the pile and typically leads to larger scour depth. The Reynolds numbers provides information on whether the flow is laminar or turbulent, and determines the characteristics of the vortex system around the pile.

Dimensionless parameters as given in Table 1 were calculated based on the equations summarized in Table 2.

OWF name	N° of OWES	Pile diameter D (m)		Scour depths S (m)	Water depths h (m)	D_{50} (μm)	Wave height $H_{s,99}$ (m)	Flow: Current Velocity $U_{c,99}$ (m/s)	Flow: Critical velocity U_{cr} (m/s)	Relative scour depths S/D	Relative water depths h/D	Froude number Fr	Reynolds number Re	Flow intensity $U_{c,99}/U_{cr}$
Robin Rigg	60	4.3	Min	1.3	5	167	2.36	1.55	0.39	0.30	1.03	0.13	$5.14x10^6$	3.51
			Max	10	14	267	2.59	1.77	0.44	2.32	3.07	0.23	$5.86x10^6$	4.43
Barrow	30	4.75	Min	0.98	15	138	2.43	0.91	0.46	0.20	3.67	0.06	$3.50x10^6$	1.89
			Max	6	23	445	2.52	1.11	0.48	1.20	4.71	0.08	$4.26x10^6$	2.40
Teesside	26	5	Min	0.65	8	51	2.52	0.54	0.42	0.13	2..08	0.04	$2.10x10^6$	1.19
			Max	1.62	20	166	2.76	0.54	0.45	0.32	3.49	0.05	$2.10x10^6$	1.29
Humber Gateway	72	4.2	Min	0.5	15	5918	2.24	1.51	1.53	0.11	3.65	0.11	$4.87x10^6$	0.58
			Max	2.51	20	19000	2.37	1.56	2.62	0.59	4.65	0.12	$5.06x10^6$	0.99
Lincs	75	5.2	Min	0.54	12	505	2.47	1.07	0.50	0.10	2.41	0.08	$4.29x10^6$	1.31
			Max	1.92	21	1982	2.71	1.67	0.86	0.38	3.88	0.13	$6.71x10^6$	3.12
Lynn and Inner Dowsing	60	4.74	Min	0.5	9	684	2.11	1.30	0.51	0.10	2.10	0.11	$4.76x10^6$	1.63
			Max	2.35	17	1950	2.36	1.45	0.80	0.49	3.47	0.13	$5.29x10^6$	2.53
Greater Gabbard	139	6	Min	0.5	23	394	2.41	1.02	0.51	0.08	3.50	0.05	$4.72x10^6$	1.14
			Max	4.54	35	2296	2.67	1.22	1.00	0.75	5.83	0.07	$5.64x10^6$	2.25
London Array	174	7	Min	1.2	1	120	1.89	0.71	0.32	0.21	0.31	0.04	$2.56x10^6$	1.14
			Max	9.5	27	930	2.36	0.81	0.61	2.02	4.67	0.19	$3.56x10^6$	2.33
Gundfleet Sands	49	4.7	Min	0.88	2	146	1.52	0.48	0.34	0.18	0.54	0.03	$1.74x10^6$	1.05
			Max	7.73	16	253	1.72	0.86	0.45	1.64	3.34	0.09	$3.12x10^6$	2.07

Table 1. Overview of studied OWFs with hydrodynamic and sedimentological site conditions.

https://doi.org/10.5194/wes-2025-41
Preprint. Discussion started: 21 March 2025

eawe european academy of wind energy
Open Access WIND ENERGY SCIENCE DISCUSSIONS

Table 2. Calculation of the variables included in the analysis

Variable	Equation	
Current velocity	$U_{c,99} = \sqrt{u_0^2 + v_0^2}$	(1)
Froude number	$Fr = \frac{U_c}{\sqrt{gh}}$	(2)
Pile Reynolds number	$Re = \frac{U_{c,99} D}{v}$	(3)
Relative density	$s = \frac{\rho_s}{\rho_w}$	(4)
Relative grain size	$D_* = \left(\frac{\rho g}{v^2}\right)^{\frac{1}{3}} D_{50}$	(5)
Critical Shields	$\theta_{cr} = \frac{0.3}{1 + 1.2D_*} + 0.55(1 - \exp(-0.02D_*)$	(6)
U_{cr}	$U_{cr} = 7 * \left(\frac{h}{D_{50}}\right)^{\frac{1}{7}} (g(s-1)D_{50}\theta_{cr})^{0.5}$	(7)
Flow intensity	$\frac{U_{c,99}}{U_{cr}}$	(8)

Sediment density (ρ_s) is 2650 kg/m^3, a value assumed for all OWFs sites based on Soulsby (1997). The water density (ρ_w), which represents sea water at the surface, is 1027 kg/m^3. The kinematic viscosity (v) is 1.3e-6 m/s^2, and the gravitational acceleration (g) is 9.8 m/s^2. Equations 4 and 6 are taken from Soulsby and Whitehouse (1997), where s represents the specific gravity of sediment grains. Equation 5 was calculated based on van Rijn (1984), where D_* is the non-dimensional grain diameter, and this is first calculated to calculate the critical Shields parameter (θ_{cr}), which corresponds to the initiation of motion at the bed. The northward (v_0) and eastward (u_0) current velocities in the water column in a temporal resolution of 1 hour are used to calculate the $U_{c,99}$.

In addition, the minimum and maximum values of the variables at each OWF are shown. The 99th quantile of significant wave heights ($H_{s,99}$) in a temporal resolution of 3 hours and current velocities ($U_{c,99}$) in a time window of 1 hour are used in this study. The 99th quantile was chosen for this study, due to scour development being more driven by largest $H_{s,99}$ and $U_{c,99}$. The datasets were obtained between pre- and post- construction bathymetries. The data were collected over a one-year period, prior to the post-construction bathymetry.

https://doi.org/10.5194/wes-2025-41
Preprint. Discussion started: 21 March 2025

eawe european academy of wind energy
Open Access WIND ENERGY SCIENCE DISCUSSIONS

Since some hydrodynamic parameters (e.g. wave period or orbital flow velocity) and geotechnical data (e.g. grain density and size distribution) were not directly available for all locations during the preparation of this study, it was not possible to determine other dimensionless parameters (Shields, KC, Ucw) that are important for the scour process with sufficient reliability.

2.3 Pre-processing of bathymetric data

Figure 2 shows the workflow used in this study, starting with the acquisition of bathymetric datasets, originally obtained from the Marine Data Exchange, and their conversion to Ordnance Datum Newlyn (ODN). This was followed by the generation of 100m x 100m tiles for each available bathymetric dataset, centered on each turbine location. If bathymetric scans with different spatial resolutions were available for the same date, only the one with the highest resolution was used. In addition, some turbine locations could not be further analysed due to missing pre-construction scans or poor data quality. Tiles with more than 50% empty cells were discarded because a high percentage of missing data increases the likelihood that important areas, such as the scour region, are poorly captured. Tests were conducted with lower missing cell thresholds (10% and 25%), but even with 50% missing data, valuable information for scour analysis was retained. Using a stricter 25% threshold, too many tiles were lost, including those that still contained useful data. As a result, 460 of the 680 turbines in the nine OWFs were analyzed in more detail.

The difference in bed elevation at turbine sites between the pre-construction (Fig 2.A) and post-construction surveys (Fig 2.B), was used for extracting scour information. The deepest scour at each turbine site was then extracted from the difference plot (Figure 2.C). A detailed description of this part of the workflow is provided in the next chapter.

https://doi.org/10.5194/wes-2025-41
Preprint. Discussion started: 21 March 2025

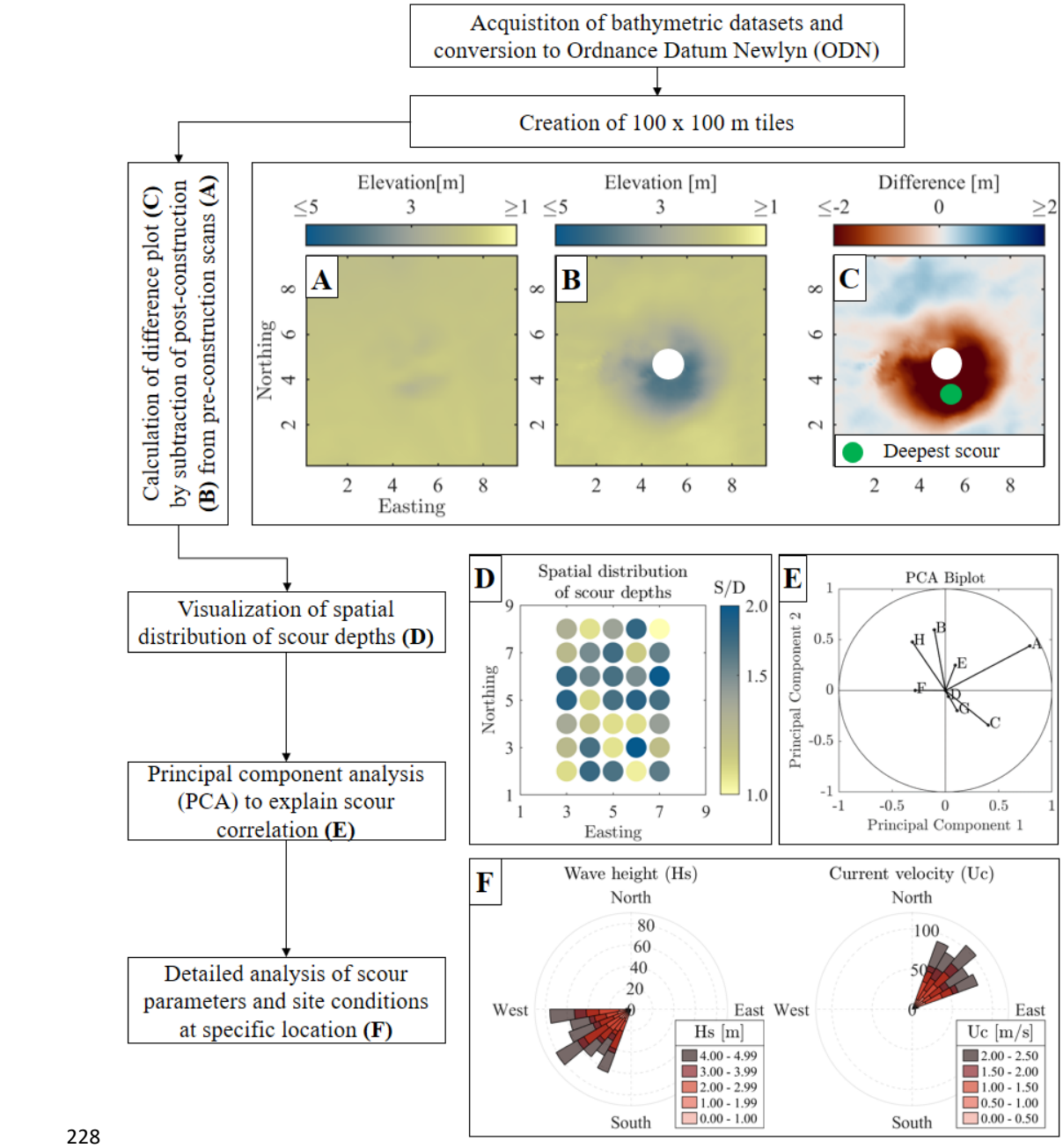

Figure 2: General workflow and methodology used to assess the scour distribution and evolution as well as the correlation between scour parameters and site conditions. A) Pre-installation scan. B) Post-installation scan. C) Difference plot after subtraction of B from –A. D) Map of spatial distribution of scour depths. E) Principal Component Analysis (PCA). F) Site conditions of wave heights and current velocities.

https://doi.org/10.5194/wes-2025-41
Preprint. Discussion started: 21 March 2025

eawe european academy of wind energy
Open Access WIND ENERGY SCIENCE DISCUSSIONS

2.4 Calculation of scour parameters

First, to eliminate outliers, a threshold based on the 99th percentile was used to filter out extreme values, ensuring that outliers did not skew subsequent analyses or visualizations. Subsequently, to address potential offsets between pre- and post-construction, a median filter was applied to both datasets. The difference in medians, excluding the presumed scour area, was considered the offset. This offset was then applied while calculating the difference plot between the pre- and post-construction bathymetries (Fig. 2A-C). To remove additional outliers close to the turbine, an area equivalent to 110% of the pile's foodprint area was excluded from the center of the difference plot.

The deepest scour depth (see green dot in Fig. 2C) was then extracted from the difference plot (Fig. 2C). The calculated scour depths were then visualized to show the spatial distribution across the nine OWFs (Fig. 2D).

2.5 Principal component analysis (PCA)

In the case of field data, the correlation of the scour process with hydrodynamic and geotechnical variables is complicated by the simultaneous change of several of these variables. In order to reduce the complexity and simplify this multivariate problem, PCA was used in a next step (Fig. 2.E). PCA works by transforming the data into a set of new variables called principal components, which are combinations of the original variables (Jolliffe & Cadima 2016). These components are ordered based on how much variance they explain, with the first principal component (PC1) explaining the maximum variance in the data, followed by the second principal component (PC2). Each component also has an eigenvalue, which shows the amount of variation it captures. Generally, the PCA is able to handle lots of independent variables and helps to simplify the data without losing important information (Harasti, 2022). Unlike studies that use PCA for variable reduction (Harasti, 2022), in our analysis we retained all principal components to identify and quantify the relationships between the selected variables.

In this study, the PCA was applied to a dataset of 692 turbines, including 177 turbines from London Array OWF and 100 turbines from Thanet OWF, based on Melling's (2015) data. The PCA was then performed using eight independent variables that contributed to the principal components. Those variables were the relative water depths (h/D), wave height ($H_{s,99}$), current velocity ($U_{c,99}$), Reynolds number (Re), Froude number (Fr), sediment size (D_{50}), flow intensity ($U_{c,99}/U_{cr}$), and the relative scour depths (S/D).

In order to correlate the relative scour depths (S/D) with the other variables, the PCA biplot was employed to estimate the correlation between the variables (Gabriel et. al., 1971). In the biplot, the angle between the respective vectors indicates the degree of correlation, with an angle close to 0° indicating a strong positive correlation, while 180° indicates a strong negative correlation and 90° indicates no correlation at all. Each correlation percentage was thus calculated by taking the cosine of the measured angle between vectors, thereby providing an estimation of how closely variables within the analysed dataset are related the relative scour depths (S/D).

An additional approach to reducing the complexity of multivariate datasets is to initially group the data based on a selected key variable. Accordingly, the PCA was also applied to the dataset after it had been grouped by grain size (D_{50} diameter) classes (Annad et al., 2021), given that the sediment characteristics of the seabed play a significant role in local scour (Qi et al., 2016). This approach facilitated a more precise estimation of local scour, thereby reducing uncertainties related to sediment.

https://doi.org/10.5194/wes-2025-41
Preprint. Discussion started: 21 March 2025

eawe european academy of wind energy
Open Access WIND ENERGY SCIENCE DISCUSSIONS

3 Results

3.1 Spatial distribution of scour depths

To illustrate the variability in scour depths between the nine studied OWFs and within single OWFs, Figure 3 shows the spatial distribution of scour depths. There are clear differences between OWFs in both the magnitude and variability of scour depths. For example, at OWF Robin Rigg (Figure 3.A), the highest scour depths were identified, the values range from 0.29 S/D to 2.49 S/D. This OWF is characterized by fine and medium sands. In contrast, the smallest scour depths occurred at the OWF of Lincs and Lynn and Inner Dowsing (Figure 3.E and 3.F), with values from 0.12 S/D to 0.92 S/D, which is possibly linked to coarse sands presented at both sites . Furthermore, the highest variability ($\sigma = 0.44$) in scour depths were detected at OWF London Array (Figure 3.H) and Barrow (Figure 3.B), likely influence by the complex seabed morphologies and sediment compositions in these areas. On the other hand, the significant variability at London Array may be explained by the presence of the Long Sand and Kentish Knock sandbank. This illustrates how different site characteristics can result in various scour distributions, even within a single OWF.

The remaining OWFs showed relatively low scour depths and little spatial variability, even though site conditions were significantly different, as indicated by their seabed conditions from very fine sand for Teesside (Figure 3.C) to coarse and very coarse gravel for Humber Gateway (Figure 3. D).

https://doi.org/10.5194/wes-2025-41
Preprint. Discussion started: 21 March 2025

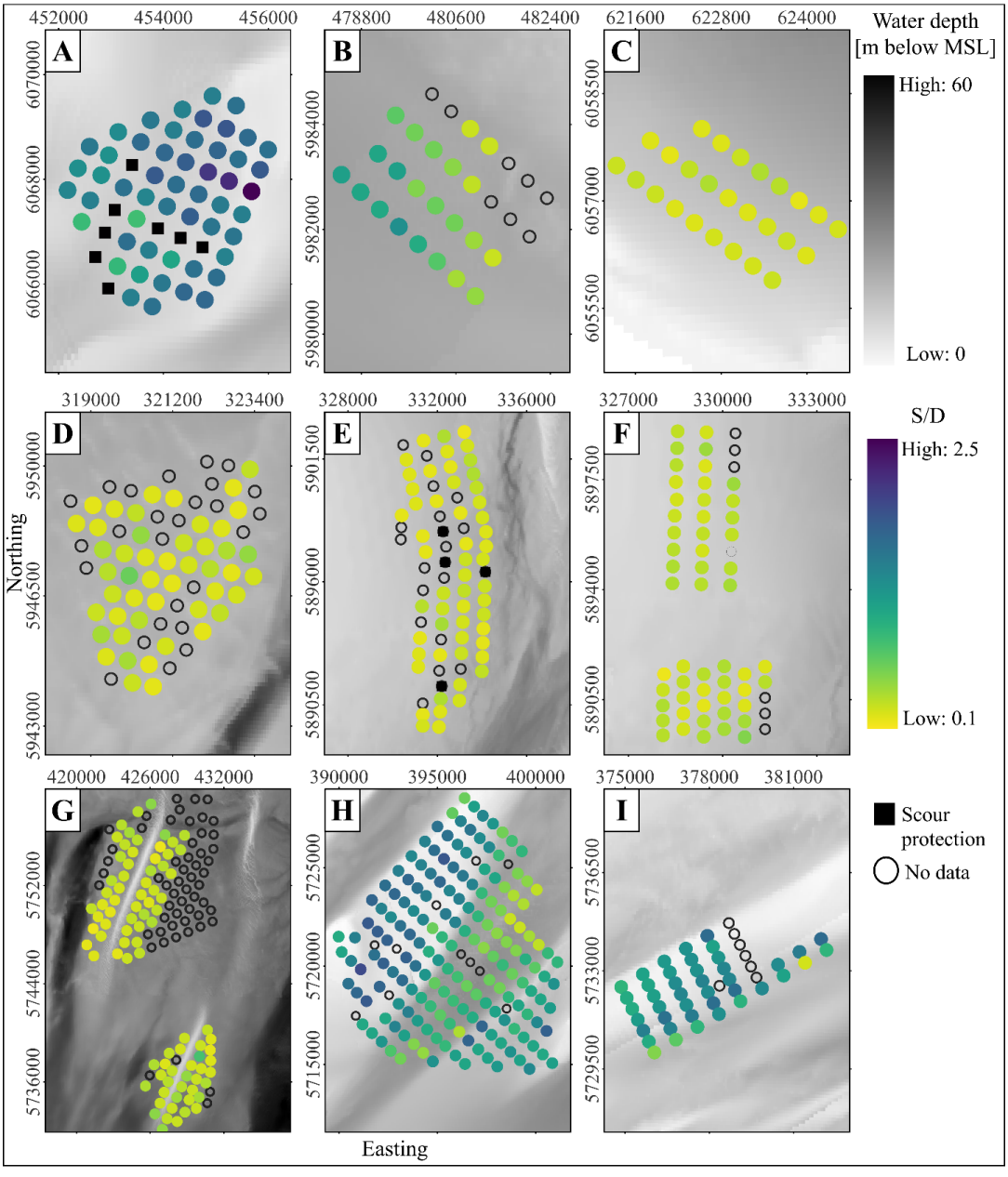

Figure 3: Spatial distribution of relative scour depths (S/D) at the nine studied OWFs. Numbered markers (1-9) denote the locations of Robin Rigg, Barrow, Teesside, Humber Gateway, Lincs, Lynn and Inner Dowsing, Greater Gabbard, London Array, and Gunfleet Sands OWFs, respectively. The upper colormap represents water depths, with darker shades indicating deeper water. The lower colormap indicates relative scour depths, with darker blue color indicating largest scour. Black filled squares represent turbines with scour protection,

https://doi.org/10.5194/wes-2025-41
Preprint. Discussion started: 21 March 2025

eawe european academy of wind energy
Open Access WIND ENERGY SCIENCE DISCUSSIONS

while empty circles denote missing data. Shown bathymetry data originates from EMODET (OBJ).https://emodnet.ec.europa.eu/en/bathymetry).

3.2 Principal component analysis (PCA)

The analysis of Figure 3 reveals notable variations in scour depths across individual OWFs. This variance underscores the need for a more detailed examination of specific wind farm characteristics to identify the drivers of scour. To this end, a PCA was conducted to correlate scour depths and selected parameters by identifying and quantifying their relationships. The PCA biplot presented in Figure 4 illustrates these correlations between scour depths and the studied variables and provides a comprehensive view of how different factors interact and influence scour depths.

a)

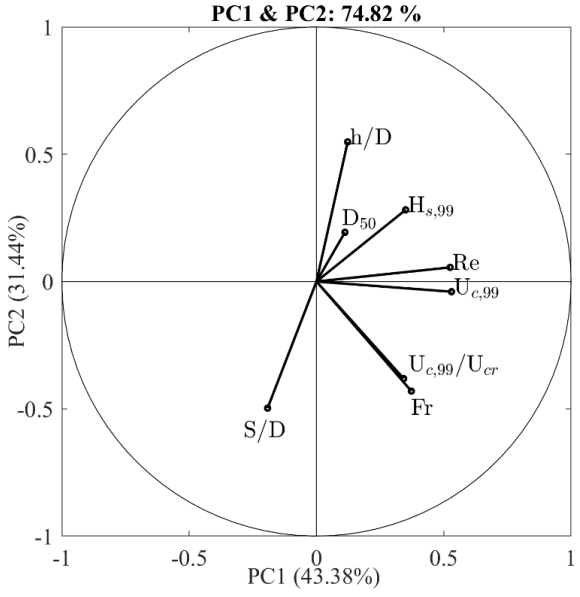

b)

Variables	θ to S/D	% Correlation with S/D
D_{50}	**171.49**	**0.989**
h/D	**171.053**	**0.988**
$H_{s,99}$	**149.91**	**0.865**
Fr	61.9	0.469
Re	117.2	0.456
$U_{c,99}/U_{cr}$	63.0	0.453
$U_{c,99}$	106.8	0.289

Figure 4: a) PCA biplot, illustrating the correlation between variables and relative scour depths (S/D). b) The table detailing the angles between S/D and the other variables, as well as their corresponding percentage correlation.

As shown in the biplot, PC1 and PC2 account for 74.82% of the variation in the data set. This high percentage indicates that these two components capture most of the significant patterns in the data, allowing for a meaningful interpretation of the relationships among the variables. In the biplot, each vector stands for a variable, with the direction and magnitude of the vector reflecting its contribution to the principal components. The variables that contribute the most to the variance in PC1 are flow velocity ($U_{c,99}$) and Reynolds number (Re), with loadings of 0.5303 and 0.5248, respectively. In contrast, the variance in PC2 is primarily explained by the relative water depths (h/D) and the relative scour depths (S/D), with loadings of 0.548 and 0.49732, respectively. This significant contribution of flow velocity ($U_{c,99}$) and Reynolds number (Re) to PC1 suggests that variations in these hydrodynamic parameters are critical in shaping the principal dynamics of the dataset.

https://doi.org/10.5194/wes-2025-41
Preprint. Discussion started: 21 March 2025

eawe european academy of wind energy
Open Access WIND ENERGY SCIENCE DISCUSSIONS

The table (Fig. 4b) next to the biplot provides further insight by showing the angular distances between the S/D vector and each of the other variables, as well as their respective correlation coefficients. One of the key observations is that despite its relatively small contribution to the total variance (as indicated by the shorter vector length in the biplot), sediment size (D_{50}) has the strongest negative correlation with scour depths (S/D), as indicated by a correlation coefficient of 0.989. This highlights the critical influence of sediment size on scour processes, even though it does not account for much of the variance captured by the first two principal components.

This observation can be explained by the underlying physical processes that affect scour depths. As noted by Whitehouse (2010) for non-cohesive sediments, larger sediment sizes are more resistant to erosion, resulting in reduced scour depths. Therefore, while $D_{50}$is strongly correlated with scour depths, it does not explain the broader variability in the data that is influenced by other factors. Variables such as flow velocity ($U_{c,99}$), Reynolds number (Re), and Froude number (Fr), although less correlated with scour depths, contribute more to the total variance. This suggests that these flow related variables influence scour depths through more complex or non-linear interactions with other hydrodynamic conditions and sediment characteristics.

Given that the initial PCA analysis indicates the strongest negative correlation between D_{50} and S/D, a more in-depths investigation of the influence of D_{50} on scour processes is required. Since the sediment characteristic of the seabed plays a significant role to local scour (Qi et al. 2016), the PCA was applied to the same data set, but pre-clustered into different soil classes (Annad et al. 2021). By reducing the uncertainties related to sediment size, this analysis should provide a better estimation of the local scour. This classification also facilitates the identification of parameters that are more influential in estimating scour for specific soil classes rather than uniformly across different types.

3.3 Principal component analysis (PCA) by clustered soil classes

https://doi.org/10.5194/wes-2025-41
Preprint. Discussion started: 21 March 2025

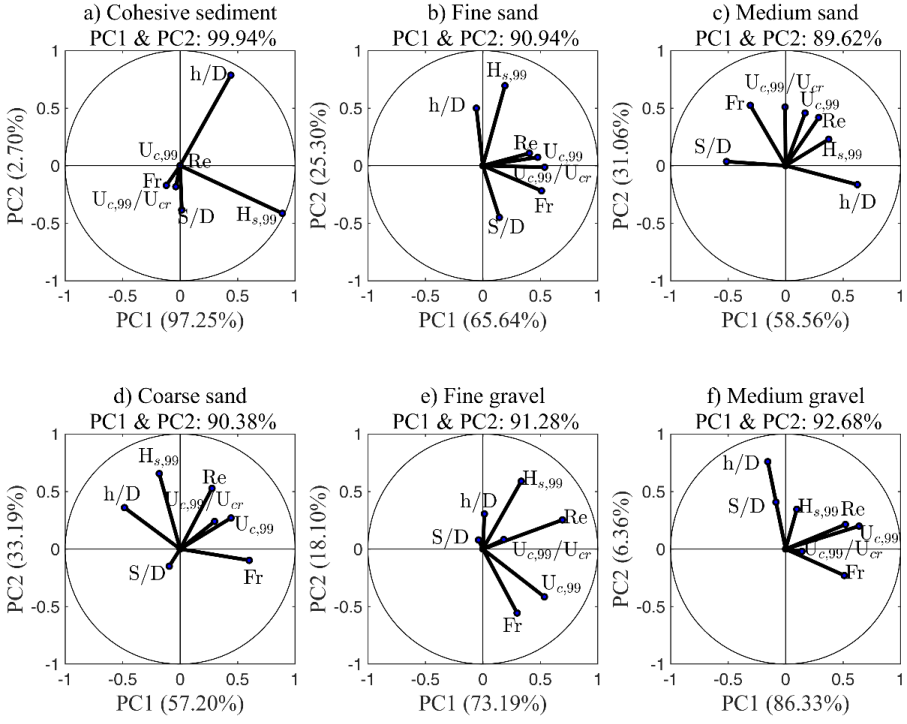

330

331 **Figure 5: PCA correlation by clustered grain size classes between the remaining 7 dimensionless parameters,**
332 **including the scour depth. a) Cohesive sediment (D_{50} ≤63 μm). b) Fine sand (63 to 200 μm). c) Medium sand**
333 **(200 to 630 μm). d) Coarse sand (630 to 2000 μm). e) Fine gravel (2000 to 6300 μm). f) Medium gravel (6300 to**
334 **20000 μm). Clustering of the grain size (D_{50}) was based on Annad et. al. (2021).**

335 Building on the initial PCA analysis, which emphasized the significant influence of grain size (D_{50}) on scour depths
336 (S/D), a more detailed investigation was conducted by categorizing the dataset into six grain size classes: cohesive
337 sediment (D_{50} ≤63 μm) with 5 data points, fine sand (63 to 200 μm) with 203 data points, medium sand (200 to 630
338 μm) with 206 data points, coarse sand (630 to 2000 μm) with 221 data points, fine gravel (2000 to 6300 μm) with 19
339 data points, and medium gravel (6300 to 20000 μm) with 73 data points.

340 Figure 5 shows PCA biplots for each soil class illustrating the relationships between scour depths (S/D) and the
341 variables h/D, $H_{s,99}$, $U_{c,99}$, Fr, Re, and $U_{c,99}/U_{cr}$. The first two principal components (PC1 and PC2) explain between
342 90.98% and 99.55% of the variance within each class, thus describing more of the variance in comparison to when the
343 PCA was applied to all data. Data complexity seems to be greatly reduced by just removing the effect of sediment. In
344 the cohesive sediment class (Figure 5a), PC1 dominates, explaining the majority of the variance, suggesting a primary
345 underlying pattern that drives the variability in scour depths. However, this result must be interpreted with caution as

https://doi.org/10.5194/wes-2025-41
Preprint. Discussion started: 21 March 2025

eawe european academy of wind energy
Open Access WIND ENERGY SCIENCE DISCUSSIONS

the analysis in this group is based on only 5 data points. In contrast, the fine sand (Figure 5b) and medium sand (Figure 5c) classes show a more balanced contribution from PC1 and PC2.

Analysis of the correlations between scour depths (S/D) and other variables within each soil class reveals different patterns. In the cohesive sediment class (D_{50} ≤63 μm), relative scour depths is positively correlated with flow intensity ($U_{c,99}/U_{cr}$). This suggests that as flow intensity increases, scour depths tends to increase, which meets physical expectations in clear water conditions, i.e. stronger flow intensity leading to larger scour (Melville, 2008). However, the data points in this cluster belong to the Teeside OWF, for which flow intensities ($U_{c,99}/U_{cr}$) between 1.17 and 1.28 m/s were determined and thus live-bed flow conditions. In contrast to clear-water conditions, the scour depths under live-bed conditions are influenced by the migration of bed forms, typically leading to scour depths smaller than that in clear-water conditions. It is important to note that the flow intensity vector ($U_{c,99}/U_{cr}$) is remarkably short, reflecting its minimal contribution to the overall variability, despite its positive correlation with scour depths (S/D). Although $U_{c,99}/U_{cr}$ is positively correlated with scour depths, its limited impact on the total variance captured by PC1 and PC2 suggests that other factors may have a stronger influence in this class.

In contrast, relative water depths (h/D) has a strong negative correlation with scour depths in fine sand (63 to 200 μm) and medium sand (200 to 630 μm). This indicates that as relative water depths increases, scour depths tends to decrease in these finer sediment classes. From a physical view, Melling (2015) found out that in similar substrates, scour depths agree well between different geographic locations. Furthermore, Melling (2015) showed that turbines located in sandy sediments seemed to show a strong influence of relative water depths on scour, insinuating that geotechnical factors are less influential in granular sediments. The decrease in scour depths with water depth seems unexpected, as in shallow water a greater water depth should lead to a larger boundary layer and thus potentially stronger horseshoe vortex and scour depths (Melville, 2008). However, as explained by Harris and Whitehouse (2014), a weaker down flow and hence a weaker horseshoe vortex can be expected in deeper water. In deeper water, the hydrostatic component of the total energy at the front of a pile becomes more significant compared to the kinetic component, resulting in a more uniform pressure field on the upstream side of the pile and a stagnation point closer to the seabed. In addition, the thinner boundary layer implied by shallower relative water depths could consequently also lead to greater bed shear stresses, resulting in generally greater sediment mobility.

The dynamics observed in coarse sand (630 to 2000 μm) and fine gravel (2000 to 6300 μm) are different from the finer sediments.

In these classes, the Reynolds number (Re) and the Froude number (Fr) show significant negative correlations with scour depth, indicating that higher values of these parameters correspond to reduced scour depth. Again, these trends are again somewhat unexpected. In coarser sediments the formation and migration of bed forms is limited, which should results in a stronger correlation with flow parameters and scour depths.

For medium gravel (6300 to 20000 μm), water depth has a positive correlation with scour depth, meaning that greater relative water depths are associated with greater scour depths in coarser sediments. The data points in the cluster can

https://doi.org/10.5194/wes-2025-41
Preprint. Discussion started: 21 March 2025

eawe european academy of wind energy
Open Access WIND ENERGY SCIENCE DISCUSSIONS

be attributed to the Humber Gateway OWF, which is the only OWF that features clear-water conditions. Given the large grain sizes, a smaller influence of flow parameters on the variability of scour depths should be expected

3.4 Correlation of scour depth with main drivers

Following the PCA (Figure 5), which identified the primary variables influencing scour depths (S/D) across sediment classes, a Pearson correlation analysis was performed to quantify the strength and direction of these relationships. Figure 6 shows the Pearson correlation results for each cluster and the variable with the strongest correlation, with the red lines representing the linear regression fit and the correlation coefficients shown in red text. The Pearson correlation was calculated by the following equation:

$$R = \frac{\sum(x_i-\bar{x})(y_i-\bar{y})}{\sqrt{\sum(x_i-\bar{x})^2 \sum(y_i-\bar{y})}} \quad \text{..... (9)}$$

Taking into account the small number of data points in this sediment cluster, scour depths at locations with cohesive sediments (Fig. 6a) show a moderate correlation between scour with flow intensity ($U_{c,99}/U_{cr}$). For the fine and medium sand clusters, the PCA revealed a similarly strong dependence of scour depth on relative water depth (h/D). Plotting scour depths against relative water depths now shows a clearer trend and hence dependence for the medium sand sites (Fig. 6c) than for the fine sand sites (Fig. 6b). The Pearson coefficients of -0.56 and -0.86 confirm this difference in the dependence of scour depth on relative water depth. The correlations of the fine and medium sand clusters are supported by a larger number of data points, increasing the reliability of the findings.

https://doi.org/10.5194/wes-2025-41
Preprint. Discussion started: 21 March 2025

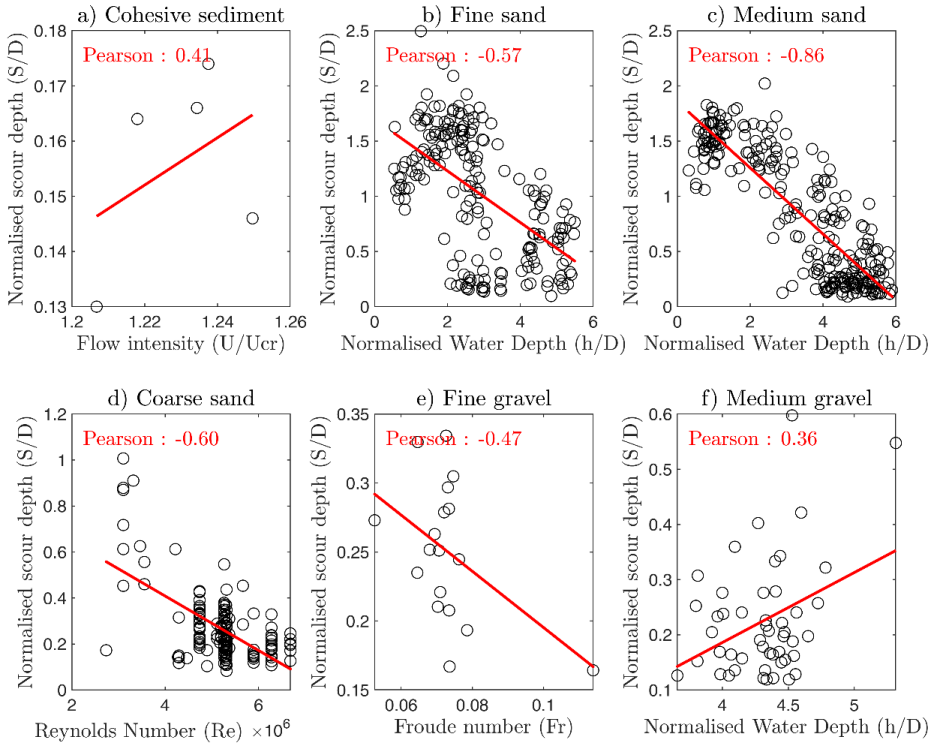

Figure 6: Pearson correlation of representative variables obtained by PCA analysis with scour depths across different grain sizes classes. a) Cohesive sediment (D_{50} ≤63 μm). b) Fine sand (63 to 200 μm). c) Medium sand (200 to 630 μm). d) Coarse sand (630 to 2000 μm). e) Fine gravel (2000 to 6300 μm). f) Medium gravel (6300 to 20000 μm).

For the coarse sand (630 to 2000 μm), the PCA analysis revealed the strongest correlations between scour depth and pile Reynolds number. The comparison of these two parameters in Figure 6d confirms the general trend that higher Reynolds numbers lead to lower scour depths, but also shows that scour depths can vary considerably within an OWF despite identical Reynolds numbers. Due to the grid size of the flow data used, the current velocities and hence the pile Reynolds numbers vary only slightly within an OWF.

For fine gravel (2000 to 6300 μm), the PCA analysis showed a very strong correlation between scour depth and Froude number. However, it is difficult to derive this trend between depth and Froude number from the comparison of these two parameters in Figure 6e. Rather, the Froude numbers for the few data points in this group of grain sizes are very close to each other, rendering the correlation unreliable.

Finally, medium gravel (6300 to 20000 μm) displays a positive correlation between scour depth and water depth, with a Pearson coefficient of 0.36. This indicates that larger relative water depths correspond to increased scour depth,

https://doi.org/10.5194/wes-2025-41
Preprint. Discussion started: 21 March 2025

eawe european academy of wind energy
Open Access WIND ENERGY SCIENCE DISCUSSIONS

although the range of this increment remains small (between 0.1 and 0.4 S/D). This variation in scour depth is relatively minor compared to the trends observed in fine and medium sands, where changes in water depth yield more pronounced differences in scour depth. The smaller impact in medium gravel may be attributed to the generally greater resistance of larger sediments to scour, even with increasing water depth.

The most significant trends emerge from the fine sand (63 to 200 μm) and medium sand (200 to 630 μm), where strong negative correlations between relative scour depths and relative water depths are observed. This suggests that significant scour occurs in shallower waters with finer sediments. Such findings highlight the importance of relative water depths as a key factor influencing scour processes in specific sediment types, emphasizing that scour management and predictions for offshore structures should take sediment characteristics and relative water depths into account. These results are consistent with the studies from Melling (2015) and Harris and Whitehouse (2014), which also show a decrease in scour depths in finer sediments as water depth increases. This negative correlation can be explained by the reduction in bed shear stress with increasing water depth, which limits sediment mobilization, particularly in fine and medium sands (Sumer & Fredsøe, 2002; Fredsøe & Sumer, 2014). However, those results are not in agreement with experimental work where scour around a monopile weakens with reducing relative water depths (e.g. May and Willoughby, 1990; Whitehouse, 1998). Consequently, relative water depths is included as a parameter in many empirical formulas, especially in for scour around bridge piles with limited water depth (eg. Laursen, 1963; Hancu, 1971; Breusers et al., 1977; May and Willoughby, 1990; Richardson et al., 2001). Besides that, these insights from field data are critical for the accurate assessment and planning of offshore infrastructure installations, particularly in regions with varying sediment characteristics.

https://doi.org/10.5194/wes-2025-41
Preprint. Discussion started: 21 March 2025

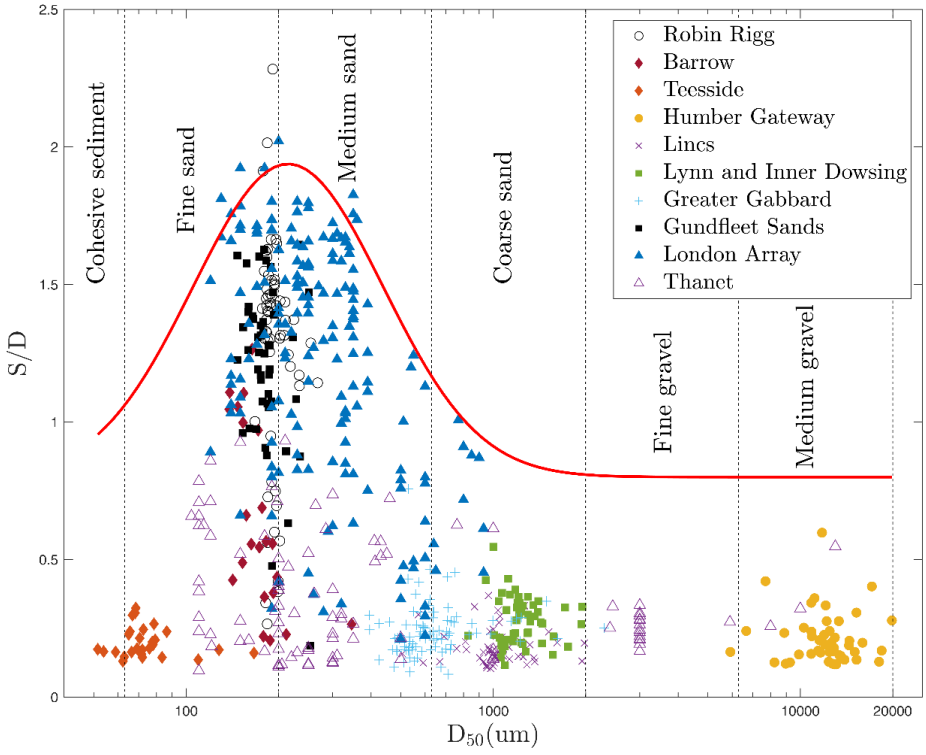

Figure 7: Relative scour depths S/D against grain size D_{50}. Red line gives approximate upper limit of S/D for various D_{50}. Data points for London Array and Thanet OWFs are included from Melling (2015).

Figure 7 summarizes the findings from the PCA analysis (Figure 4) by plotting the relationship between the relative scour depth (S/D) and grain size D_{50} across all the sampled locations. This figure illustrates a discernible trend where the largest scour depths scour occur predominantly in fine to medium sands, as indicated by the Gaussian fit line which approximates the upper limit of S/D for various D_{50}. This visualization captures the broad distribution of data points and highlights the significant influence of grain size on scour depths, confirming the results PCA of the PCA that identified D_{50} as a key factor in scour dynamics. The trend shown in Fig. 7 is well explained. In general, the mobility potential of the sediments decreases with increasing grain size, which leads to lower scour depths for coarser sediments. Very fine sediments, on the other hand, are subject to the influence of cohesion forces that reduce their erodibility, which also leads to lower scour depths. Therefore, fine and medium sandy sediments have the largest scour potential, which is reflected in the data of Fig. 7. The different symbols represent the OWF, highlighting the geographic spread and variability within the dataset. However, it is important to note that the majority of the data points fall within the range of fine to medium sands, potentially skewing the interpretation.

https://doi.org/10.5194/wes-2025-41
Preprint. Discussion started: 21 March 2025

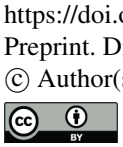

eawe european academy of wind energy
Open Access WIND ENERGY SCIENCE DISCUSSIONS

452 .

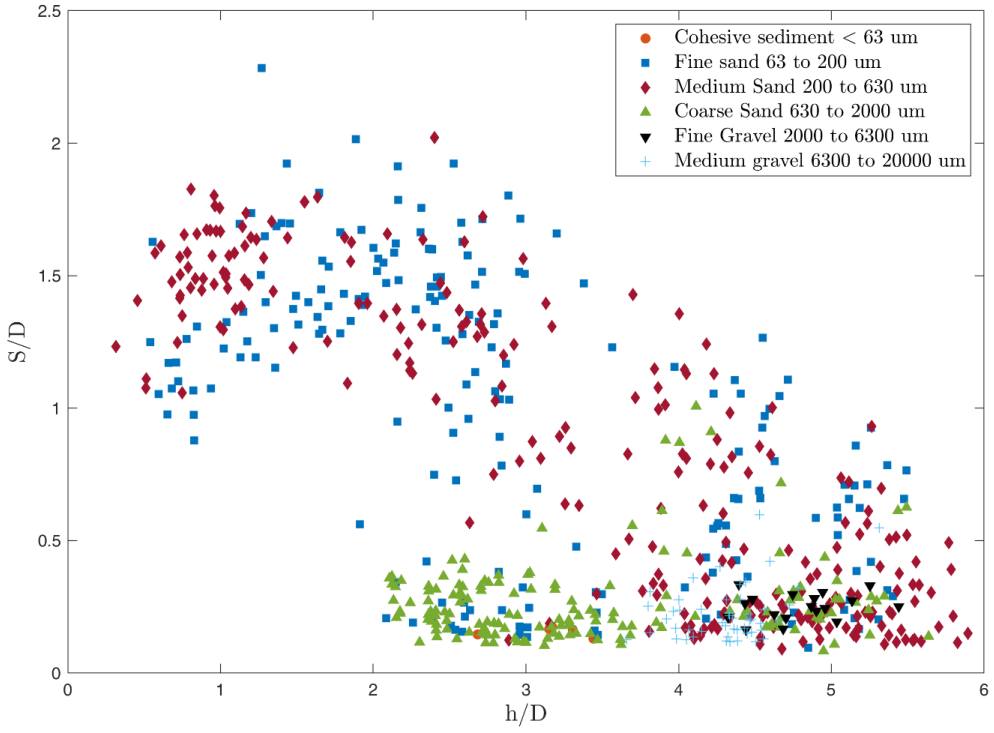

453

454 **Figure 8: Relative scour depths vs relative water depths, and sediment classification. Data points for London**
455 **Array and Thanet OWFs are included from Melling (2015).**

456 In addition to the influence of sediment grain size, relative water depth has been shown to be the most important factor
457 influencing relative scour depth. However, it should be noted that water depth has a direct effect on other parameters.
458 For example, not only is the Froude number formed with water depth, but water depth also significantly determines
459 the potential influence of waves on the development of scour, which in this study has so far only been considered via
460 the significant wave height. It is therefore not clear whether the influence of water depth on scour depth is a causal
461 factor, or whether the cause of changes in scour depth is related to changes in flow conditions caused by changes in
462 water depth. Nevertheless, Figure 8 illustrates the comprehensive correlation between the relative scour depth (S/D)
463 and the relative water depth (h/D), with the differently colored points representing the studied sediment clusters.

464 The trend observed figures 6b and 6c is reaffirmed in Figure 8. A distinct relationship exists between the scour depth
465 and water depth in these two sediment types, i.e. both fine sand (63 to 200 μm) and medium sand (200 to 630 μm)
466 show that the scour depth decreases with increasing water depth. This trend appearing throughout the bigger dataset
467 emphasizes strong negative correlation between water depth and scour depth for those sediment classes. This behavior

https://doi.org/10.5194/wes-2025-41
Preprint. Discussion started: 21 March 2025

is consistent with findings from previous analyses that identified water depth as a critical factor in shaping scour dynamics (Whitehouse et al., 2010 and Melling et al., 2015).

In contrast, for sediments with median grain diameters above coarse sands ($D_{50} \geq 630\ \mu m$) the scour depth remains relatively constant and shows little variability. Figure 8 suggests a generally stable relationship between scour depth and water depth for these sediment classes, where changes in water depth do not significantly alter scour depth. However, there are a few exceptions. For example, some locations with coarse sand located in deeper water exhibit unexpectedly large scour depths. These outliers might stem from site-specific conditions such as dynamic sandbanks and highly variable, as seen at the London Array OWF (Sturt et al., 2009). These unique environments, characterized by flow recirculation and sediment mobility, can lead to deviations from expected scour behavior (Melling et al., 2015). The results for fine and medium sands suggest a potential influence of water depth in reducing scour depth, which could have implications for sediment transport and the marine environment. Although these results are preliminary, they provide a first step in understanding how offshore wind turbines could affect sediment redistribution in regions dominated by these sediment types and small water depth.

3.5 Detailed analysis of scour patterns for selected OWFs

Following the observed overall trend shown in Figure 8, this section moves on to examine scour patterns within individual OWFs, such as Robin Rigg, Lynn and Inner Dowsing, and London Array. This specific analysis will assess whether the global relationship between scour depths, D_{50}, and relative water depths holds under the unique environmental conditions of each site. This section aims to further our understanding of the dynamics between sediment characteristics and scour processes by a detailed analysis of the variation within each wind farm to determine if these global correlations are consistent at the local scale or if there are deviations due to site-specific factors.

3.5.1 Robin Rigg OWF

Robin Rigg is presented and discussed in this section as this OWF has the largest overall scour depths of all the OWFs. This detailed analysis will help to investigate whether the negative correlation between S/D and h/D observed globally in Figure 8 holds true under variable geotechnical conditions, taking into account that sediment grain sizes range from fine to medium sands.

Figure 9 shows the distribution of scour depths at Robin Rigg in relation to the variable geotechnical and hydrodynamic site conditions. This sequence begins with Figure 9A, showing the spatial distribution of scours measured one year after turbine installation. A significant variation in scour depths in different areas of the OWF can be observed, with the deeper scour depths mainly located in the northeastern part, particularly around turbines D7, C6, B5 and B4, which are located in the shallowest waters. Figure 9B shows the spatial distribution of the median grain diameter D_{50} in the uppermost sediment layer in 2005, with sediment sizes predominantly in the range of fine to middle sand (182 µm to 268 µm). Turbines in areas with finer sands, such as D4, D5, and D6, are observed to generally experience the large scour, consistent with previous observations by Whitehouse (2006) that finer sand substrates are more susceptible to scour.

https://doi.org/10.5194/wes-2025-41
Preprint. Discussion started: 21 March 2025

eawe european academy of wind energy
Open Access WIND ENERGY SCIENCE DISCUSSIONS

Figure 9C shows the correlation of S/D and h/D, classified by colored points which represent sediment grain size from figure 9B. Contrary to the clear negative correlation between S/D and h/D observed globally in Figure 8, Figure 9C shows a wide distribution of data points with no clear trend, suggesting that local factors in addition to relative water depths and sediment type have an influence on scour at this site.

For additional insight, Figures 9D and 9E show the distribution of the directions of significant wave heights, as well as the directions of current velocity magnitudes one-year period, prior the post scan. The highest wave heights came predominantly from the southwest, which should influence sediment mobility and thus scour structures along this direction and especially in shallow water depths where wave-induced shear stresses should be higher. Similarly, the tidal current, with its main directions of south-west and north-east, should result in a change in scour depths along this main axis. However, a clear trend of scour depth changing in this direction is not given for Robin Rigg.

.

https://doi.org/10.5194/wes-2025-41
Preprint. Discussion started: 21 March 2025

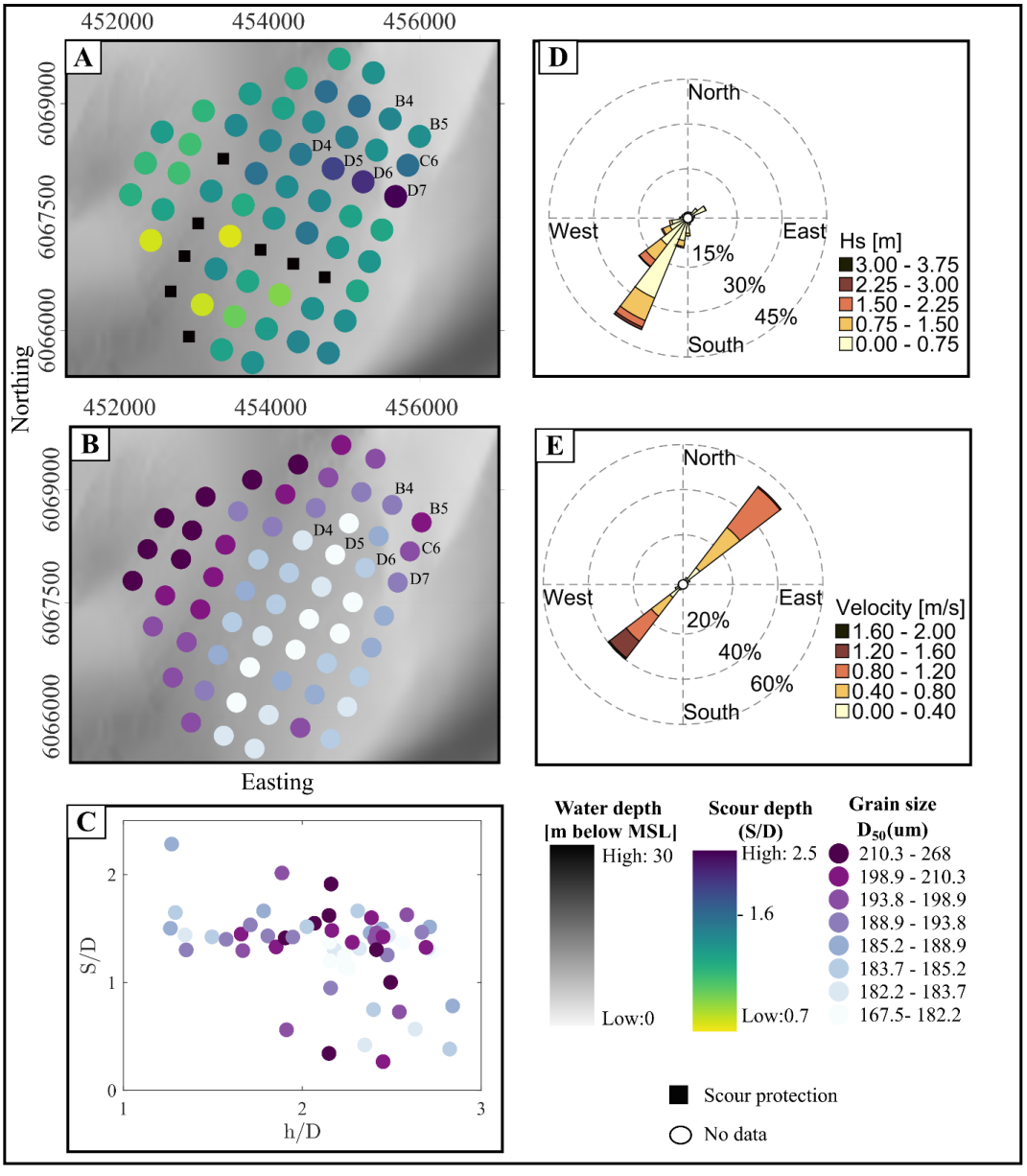

Figure 9: A) Spatial distribution of relative scour depths (S/D) from 2008-2009 at Robin Rigg OWF. B) Grain-size distribution. C) Relative scour depths vs relative water depths, and grain size classification D) Significant wave heights E) Current velocities.

This comprehensive analysis using Figures 9A to 9E shows that while trends obtained from global findings provide a useful baseline for understanding scour, the actual scour observed at Robin Rigg does not necessarily follow those trends. While the distribution of scour depths appears to be strongly influenced by local environmental conditions such

https://doi.org/10.5194/wes-2025-41
Preprint. Discussion started: 21 March 2025

as sediment type, waves and currents, the dominant influence among these cannot be clearly identified, rather the distribution of scour depths appears to be due to the interaction of all influences.

The discrepancies between the local scour behavior at Robin Rigg and the broader trends observed in Figure 8 underscore the need for site-specific assessments. Such detailed analyses are critical to the development of effective scour management and mitigation strategies tailored to the unique conditions of each offshore wind farm.

3.5.2 Lynn and Inner Dowsing OWF

Lynn and Inner Dowsing was chosen as a further example as this OWF had the lowest scour depths of all the OWFs investigated and is also characterized by coarse to very coarse sands. Figure 10 provides the same analysis as Figure 9 by providing insight into how local conditions compare to the global trend seen in Figure 8. Figure 10A shows the spatial distribution of relative scour depths (S/D) measured from 2007 to 2010. Figure 10A shows that the largest scour depths are mainly concentrated in the Inner Dowsing area, especially around turbines ID1, ID2, ID8, ID9, ID12, ID24, and ID30. Except for turbine L21, which has the deepest scour depths in the entire wind farm and which is located at the southeastern end. The significant scour depths observed at certain locations (e.g., D30, L21) are related to cable exposure (EGS Ltd, 2012; EGS Ltd, 2013), while smaller scour depths are more common in the southern region. Overall, the spatial distribution shows a slight trend of increasing scour depths from south to north.

https://doi.org/10.5194/wes-2025-41
Preprint. Discussion started: 21 March 2025

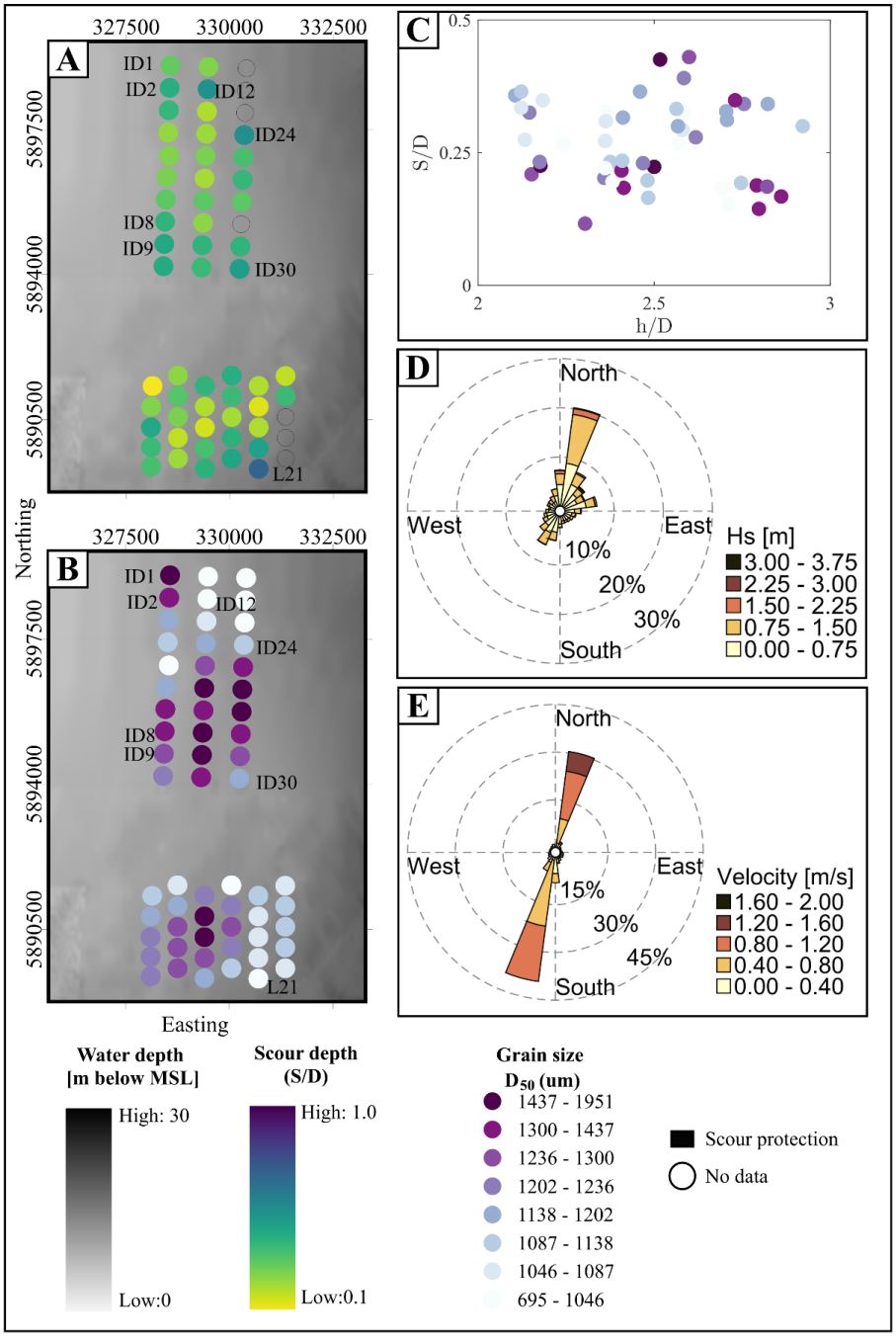

536

537 **Figure 10: A) Spatial distribution of relative scour depths (S/D) at Lynn and Inner Dowsing OWF from 2007-**
538 **2010. B) Grain-size distribution. C) Relative scour depths vs relative water depths, and grain size classification.**
539 **D) Significant wave heights E) Current velocities.**

https://doi.org/10.5194/wes-2025-41
Preprint. Discussion started: 21 March 2025

Continuing with the spatial overview, Figure 10B introduces the spatial distribution of D_{50} median grain sizes, which shows a range from coarse to very coarse sands (695 to 1951 μm).. The correlation between relative scour depth (S/D) and relative water depth (h/D) is examined in Figure 10C. Similar to Robin Rigg, this OWF does not display the negative correlation as seen globally in Figure 8, suggesting that additional local factors may significantly influence scour depths.

Consequently, the significant wave heights and current velocities from hindcast data are shown in Figure 10D and 10E. The highest wave heights, observed from the northeast, and strong tidal currents flowing from southwest to northeast, highlight the dynamic environmental forces at play. The presence of the largest scour depths in the Inner Dowsing area align with the direction of the highest tidal current velocities (Fig. 10E) recorded in the northeast part as well the main direction of waves. Therefore, the direction of both tidal current and waves likely play a significant role for the scour development in this wind farms, as the seabed conditions and water depth locally do not exhibit a distinct correlation.

3.5.3 London Array OWF

Following the previous results, the analysis for London Array OWF shows a wide range of scour depths from 0.2 S/D to 2.1 S/D. This variability differs markedly from the consistently larger scour depths observed at Robin Rigg and the limited maximum depths of up to 1.0 S/D at Lynn and Inner Dowsing. "The area of London Array OWF is characterized by an alternating pattern of deep channels (Black Deep, Knock Deep) and sandbanks (Long Sands, Kentish Knock). These topographic features significantly contribute to the local scour patterns. Water depths at this site range from 0 to 30 m, with Long Sands known for its significant variations in bed elevation but general stability of position. Meanwhile, Knock Deep is notable for its eastward shift over time, which has widened the channel and maintained a constant bed level.

https://doi.org/10.5194/wes-2025-41
Preprint. Discussion started: 21 March 2025

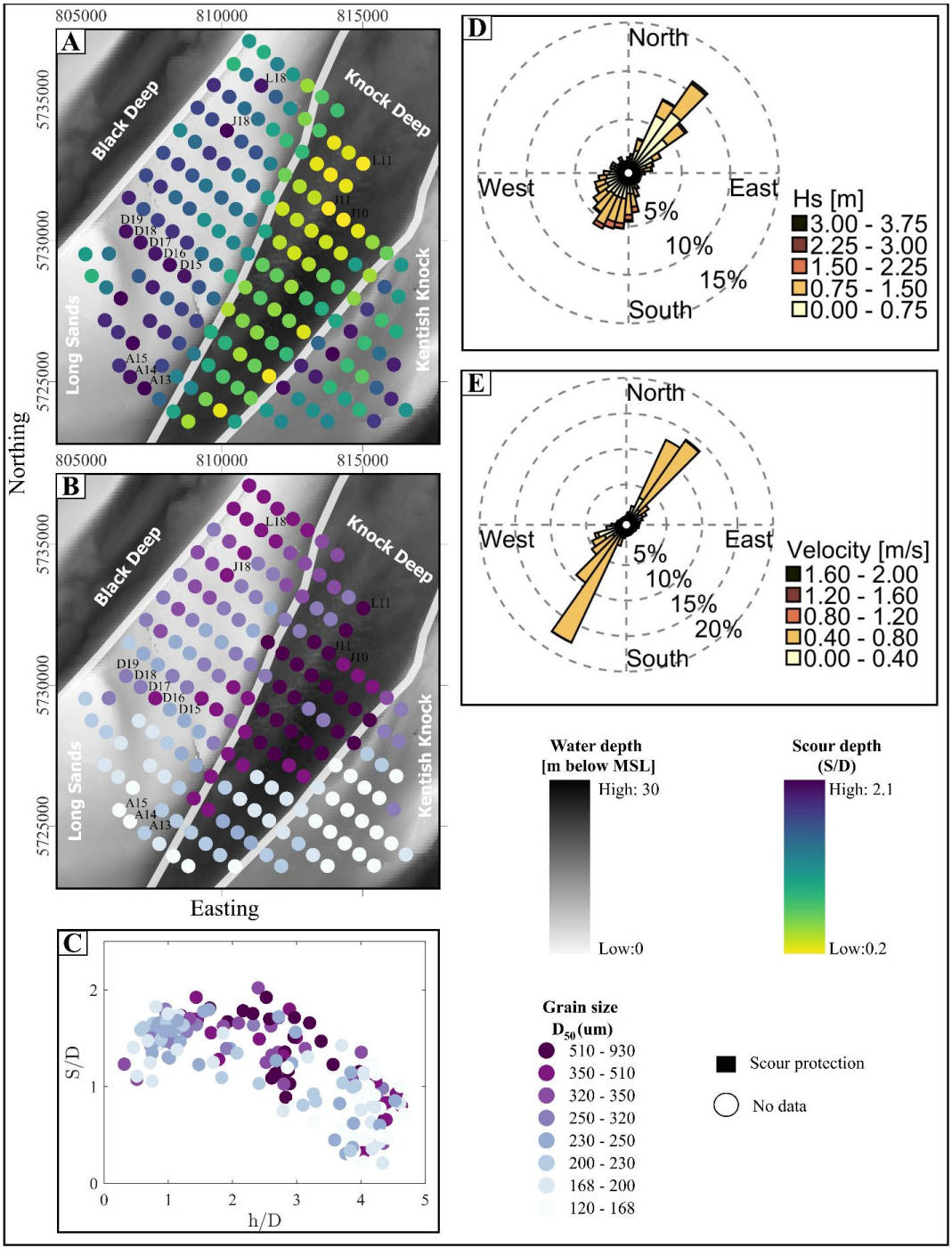

560

https://doi.org/10.5194/wes-2025-41
Preprint. Discussion started: 21 March 2025

eawe european academy of wind energy
Open Access WIND ENERGY SCIENCE DISCUSSIONS

Figure 11: A) Spatial distribution of relative scour depths (S/D) at London Array OWF from 2010-2014. B) Grain-size distribution. C) Relative scour depths vs relative water depths, and Grain size classification. D) Significant wave heights and E) Current velocities. S/D and D_{50} data are used from Melling (2015)

In Figure 11A, the distribution of scour depths shows that the variation in scour is strongly influenced by the underlying topography, with significantly greater scour depths on the sand banks compared to the channel. Addionally a trend of increasing scour depths is observed from northeast to southwest, which is particularly notable in the channel area. The smallest scour is observed in the northern part of Knock Deep with a ratio of 0.2 S/D and the largest in the southern part of Long Sands with 2.1 S/D. The differences in scour depths can be derived directly from the seabed topography, with greatest average scour depths found in the Long Sands with 1.53 S/D, followed by Kentish Knock (S/D = 1.37), and then Knock Deep (S/D = 0.77) with the smallest average. The sediment distribution across this OWF, shown in Figure 11B, ranges from very fine to coarse sands. Coarse sands can be found in Knock Deep, where generally the smallest scour depths are seen (e.g., L11, J10 and J11). Furthermore, the largest scour depths are noticed in the southern part of Long Sands (e.g. A13-A15, D15-D19, J18 and L18), where the sediment varies from very fine to fine medium sands. There is therefore a reasonable correlation between grain size and scour depth, which is consistent with the previously observed global trend. Additionally, Figure 11C shows a negative correlation between S/D and h/D aligning with the global trend observed in Figure 8, i.e. that shallower relative water depths can be associated with deeper scour, while deeper waters tend to have reduced scour depths. This trend may be explained by the findings of Hjort (1975), who demonstrated that bed shear stress decreases with increasing water depth for the same flow and structure diameter, potentially leading to reduced scour at greater depths. However, as the water depth in the London Array OWF changes simultaneously with the sediments, i.e. coarser grained sediments are present in the deeper water depths of Knock Deep, the cause of the different scour depths cannot be clearly attributed to either the sediments or the water depth. Other hydrodynamic, environmental, and topographic factors also play a critical role in shaping these patterns at this OWF, underscoring the complexity of the influences involved.

Significant wave heights and current velocities, as shown in Figures 11D and 11E, provide important insights into the scour dynamics at the London Array. These figures show that, in addition to relative water depths and sediment grain sizes, wave and current dynamics might be critical factors at this wind farm. The predominant direction of both waves and currents is northeast to southwest, consistent with the estuarine influence of the area, where river discharge also significantly affects hydrodynamic conditions. This influence is particularly evident at the Long Sands and Kentish Knock sandbanks, which are shaped by the combined action of waves and currents (London Array Ltd, 2005).

Figure 11D shows that the highest wave heights are observed coming from the northeast, with values exceeding 3.0 m, and lower wave heights propagating from the southwest. This gradient in wave height suggests a correlation with increased scour depths in regions exposed to higher wave energy, suggesting a strong link between wave dynamics and seabed modification. Similarly, Figure 11E highlights a larger number of strong currents coming from the southeast. These higher velocities correspond to areas with more pronounced scour depths, highlighting the role of strong currents in influencing sediment transport and depositional patterns.

https://doi.org/10.5194/wes-2025-41
Preprint. Discussion started: 21 March 2025

In addition, the local tidal dynamics vary significantly across the wind farm, with the flood tide dominating the southern banks and the ebb tide more influential on the northern banks (Kenyon and Cooper, 2005). This variation is due to the sheltering effect of the sandbanks, which are slightly offset from the orientation of the ebb tide, and is particularly pronounced at Long Sands (London Array Ltd, 2005). The interplay of river discharge, wind stress, tidal surge and density driven currents follow the pathways created by the existing topography, further complicating the hydrodynamic environment and its effect on scour at the London Array OWF.

After analyzing the scour depths at 9 wind farms and with different ranges of scour depths, the variation of scour depths can also be noticed in individual OWFs, as in the case for London Array OWF.

4. Implications for scour predictions for OWFs

Overall, this study extends the investigation of scour dynamics to a regional scale by analyzing correlations between relative scour depth and site conditions across multiple OWFs to identify consistent scour patterns and trends. The analysis highlights a significant correlation between larger scour depths and finer sediment types (particularly fine and medium sands), a finding consistent with sediment transport theories that suggest finer noncohesive grains are more susceptible to mobilization by hydrodynamic forces. This broad correlation, observed across different geographic locations and environmental conditions, reinforces the universality of sediment size as a fundamental factor in scour processes, as documented in the extensive work of Vanhellemont et al. (2014) and Rivier et al. (2016). Given the large underlying database, this study adds weight to the argument for the universal incorporation of detailed sediment characteristics into scour assessment practices.

However, the analysis also showed that the strong influence of the erosion potential of the sediments in the field alone cannot describe all observations. The PCA analysis also provided a strong negative correlation observed between relative scour depth(S/D) and relative water depth (h/D), particularly in fine and medium sand sediments, suggesting that the relative water depth (h/D) plays a critical role in scour processes, confirming the trends observed by Whitehouse et al. (2010) and Melling et al. (2015) for field data. The decrease of the scour depth with decreasing water depth seems unexpected and contradicts common scour prediction approaches like e.g. Breusers et al. (1977), which however are often derived for flow conditions with shallow water depth. Harris and Whitehouse (2014) argued that in deeper water, a weaker downflow and hence a weaker horseshoe vortex can be expected, ultimately leading to smaller scour depth. As the depth increases, the hydrostatic component of the total energy at the front of the pile increases relative to the kinetic component. Additionally, the reduction in boundary layer thickness, induced by decreased water depths, has the potential to enhance bed shear stresses, thereby increasing sediment mobility. For certain sediment groups, the PCA demonstrated a stronger correlation with the pile Reynolds number or the Froude number. This finding underscores a complex dynamic that is frequently oversimplified in existing models. The results indicate a necessity to incorporate nonlinear hydrodynamic models into scour prediction frameworks. The results of the PCA reveal the necessity for a diversified approach to the modeling of scour in complex field conditions, which extends beyond the scope of traditional uniform applications.

This analysis demonstrates that individual OWFs exhibit unique environmental and sediment conditions, which can either amplify or moderate broader trends. The London Array OWFs serves as a prime example of the predictive reliability of observed regional trends, as local data closely mirrors general trends. Conversely, sites such as Robin Rigg and Lynn and Inner Dowsing exhibit deviations from these trends due to their distinct sediment compositions

https://doi.org/10.5194/wes-2025-41
Preprint. Discussion started: 21 March 2025

eawe european academy of wind energy
Open Access WIND ENERGY SCIENCE DISCUSSIONS

and hydrodynamic conditions, underscoring the necessity for site-specific adjustments to scour prediction models. These findings underscore the intricacy of employing global models on a local scale and underscore the significance of site-specific data in validating and refining these models to enhance their accuracy and applicability.

5 Limitations and future research

Although this study provides a detailed analysis of scour depths at nine OWFs, certain limitations must be addressed to improve the interpretation of the findings. Although the dataset spans multiple years, it represents snapshots in time and may not fully capture the dynamic evolution of scour processes under fluctuating metocean conditions (Matutano et al., 2013; Carpenter et al., 2016). Hindcast data, while valuable for long-term trends, are often based on limited spatial resolution that may underestimate short-term extreme events such as storm surges or localized current variations (Whitehouse et al., 2010; Sturt et al., 2009).

Using PCA is effective in identifying dominant linear relationships between scour depths and key variables; however, it may miss critical nonlinear interactions that drive scour processes (Schendel et al., 2020; Lyu et al., 2021). Parameters such as the KC number and Shields parameter, which account for sediment motion initiation and hydrodynamic forces, could not be reliably determined in this study due to data limitations. Given their importance in understanding sediment transport and scour development (Sheppard et al., 2004; Zhao et al., 2012), future studies should prioritize the inclusion of these dimensionless parameters to provide a more robust assessment and comparison of scour processes.

The next step in this research is to develop data-driven models and investigate the broader implications for regional sediment dynamics. Future studies will focus on OWFs located in fine and medium sands where significant scour activity is observed. By focusing on these environments, we aim to improve prediction capabilities and better understand the mechanisms that drive scour, particularly in areas that are susceptible to substantial sediment mobilization.

Finally, while the present study focused on localized scour processes, the cumulative effects of OWF structures on regional sediment transport and marine ecosystems remain a significant knowledge gap (Christiansen et al., 2022; Schultze et al., 2021). Future research must employ interdisciplinary methodologies to rigorously assess the ecological impacts of sediment mobility and scour on marine habitats. By integrating regional sediment transport models with comprehensive ecological assessments, we can optimize offshore wind energy development to meet both sustainability and environmental protection goals, ensuring long-term benefits for infrastructure resilience and marine ecosystem health.

6 Conclusion

Achieving the European Union's (EU) offshore wind energy targets requires development of OWFs in regions with diverse and often poorly understood meteoceanic and geophysical conditions. However, this demand underscores critical knowledge gaps regarding the interaction of these installations with the marine environment, particularly with respect to scour processes and sediment mobilization. A comprehensive understanding of scour dynamics is essential, not only to ensure structural integrity, but also to assess potential impacts on regional sediment transport and broader ecosystem functions.

https://doi.org/10.5194/wes-2025-41
Preprint. Discussion started: 21 March 2025

eawe european academy of wind energy
Open Access WIND ENERGY SCIENCE DISCUSSIONS

In this study, high-resolution bathymetry data were used to analyze field-measured scour depths of 460 monopiles across nine British OWFs. The analysis included a PCA in which eight hydrodynamic and geotechnical variables were considered to identify the dominant driver influencing scour depths variability. This analysis provided a basis for understanding the primary correlations between scour depths and metocean site conditions, but also highlighted the complexity of these relationships, requiring further refinement.

The main conclusions can be summarized as follows:

(1) **Universal drivers of scour:** Across all nine OWFs, the PCA identified D_{50}, as one of the main drivers in influencing scour depths variability, together by the relative water depths (h/D). The analysis across all OWFs (Fig. 8) showed that greater scour depths occurred in shallower waters, particularly at location with sediments composed of (63 to 200 μm) and medium sand (200 to 630 μm). This result highlights the critical role of sediment size in scour formation and confirms that finer sediments are more susceptible to hydrodynamic forcing.

(2) **Sediment-specific trends:** In order to explore the variability within sediment types, the data set was clustered according to D_{50}, and a PCA was applied to each cluster. For fine sand (63 to 200 μm) and medium sand (200 to 630 μm), relative water depths was found to be the dominant driver of scour depths, demonstrating the sensitivity of these sediment types to hydrodynamic forcing in shallower relative water depths. For coarser sediments, such as coarse sands (630 to 2000 μm) and fine gravels (2000 to 6300 μm), the correlations were less pronounced, reflecting a greater resistance to scour. This sediment-specific analysis highlights the importance of considering sediment type when assessing scour susceptibility and designing OWFs, and how different sediment types can influence sediment transport patterns.

(3) **Site-specific variability:** Due to local factors such as sediment conditions, hydrodynamic conditions, and topography, individual OWFs exhibited unique scour depths patterns. For example, London Array (Fig. 11C) showed trends similar to the global results (Fig. 8), with relative water depths and site topography as the primary influences on scour, followed by current and wave conditions. In contrast, OWFs such as Robin Rigg and Lynn and Inner Dowsing showed no discernible trends between scour depths and the key drivers obtained from the global PCA, highlighting the need for individual analyses to account for local complexities.

This study also highlights the potential environmental impacts of scour-induced sediment transport. While the primary focus was on identifying the physical drivers of scour, the findings could provide a first step in assessing potential impacts of OWF on the marine environment due to a changed regional sediment mobility. The entrainment of eroded sediment into the water column, with subsequent long-range transport, raises concerns about sediment deposition and potential impacts on benthic habitats and marine wildlife in far-field regions.

Future research should prioritize the refinement of predictive scour models that incorporate temporal data and expanded hydrodynamic parameters to improve accuracy in diverse sedimentary environments. In addition, integrated approaches that combine regional sediment transport modeling with ecological assessments are critical for evaluating

https://doi.org/10.5194/wes-2025-41
Preprint. Discussion started: 21 March 2025

eawe european academy of wind energy
Open Access WIND ENERGY SCIENCE DISCUSSIONS

the cumulative impacts of OWF facilities on marine ecosystems. These efforts will facilitate the development of sustainable OWF designs that minimize environmental disturbance while advancing renewable energy goals.

Data availability: The data set used in this study is available in the Marine Data Exchange (MDE) (https://www.marinedataexchange.co.uk/) and by the Copernicus Marine Service (CMEMS) (https://marine.copernicus.eu/)

Authors contribution: K. G.: Writing – original draft preparation, visualization, formal analysis, conceptualization, methodology. **C.J.** Writing – review & editing, supervision, conceptualization, project administration. **G.M**. Writing – review & editing, resources. **A.S.** Writing – review & editing, methodology. **M.W**. Writing – review & editing, Supervision. **T.S.** Writing – review & editing, Funding acquisition, Supervision.

Competing interests: The authors declare that they have no conflict of interest**.**

Acknowledgements: This work contributes to the DAM Research Mission sustainMare and the project CoastalFutures (Project Number: 03F0911G) funded by the German Federal Ministry of Education and Research (BMBF). The responsibility for the content of this publication lies with the authors.

References

Annad, M., Lefkir, A., Mammar-Kouadri, M., & Bettahar, I. (2021). Development of a local scour prediction model clustered by soil class. Water Practice & Technology, 16(4), 1159-1172.

Baykal, C., Sumer, B. M., Fuhrman, D. R., Jacobsen, N. G., & Fredsøe, J. (2015). Numerical investigation of flow and scour around a vertical circular cylinder. Philosophical Transactions of the Royal Society A: Mathematical, Physical and Engineering Sciences, 373(2033), 20140104.

Baelus, L., Bolle, A., & Szengel, V. (2018). Long term scour monitoring around on a sandy seabed. In Scour and Erosion IX: Proceedings of the 9th International Conference on Scour and Erosion (ICSE 2018), November 5-8, 2018, Taipei, Taiwan,CRC Press.

Baeye, M., & Fettweis, M. (2015). In situ observations of suspended particulate matter plumes at an offshore wind farm, southern North Sea. Geo-Marine Letters, 35, 247-255.

Bailey, H., Brookes, K.L., Thompson, P.M., 2014. Assessing environmental impacts of offshore wind farms: lessons learned and recommendations for the future. Aquat. Biosyst. 10, 1–13. https://doi.org/10.1186/2046-9063-10-8.

Bolle, A., De Winter, J., Goossens, W., Haerens, P., & Dewaele, G. (2012, August). Scour monitoring around offshore jackets and gravity based foundations. In Proceedings of the Sixth International Conference on Scour and Erosion, Paris, France (pp. 27-31).

Breusers, H. N. C., Nicollet, G. and Shen, H. W. (1977). Local Scour Around Cylindrical Piers, Journal of Hydraulic Research 15(3): 211{252.

https://doi.org/10.5194/wes-2025-41
Preprint. Discussion started: 21 March 2025

Brignon, J.M., Lejart, M., Nexer, M., Michel, S., Quentric, A., Thiebaud, L., 2022. A risk- based method to prioritize cumulative impacts assessment on marine biodiversity and research policy for offshore wind farms in France. Environ. Sci. Pol. 128, 264–276. https://doi.org/10.1016/j.envsci.2021.12.003.

Carpenter, J. R., Merckelbach, L., Callies, U., Clark, S., Gaslikova, L., & Baschek, B. (2016). Potential impacts of offshore wind farms on North Sea stratification. PloS one, 11(8).

Carreiras, J., Larroudé, P., Seabra-Santos, F., & Mory, M. (2001). Wave scour around piles. In Coastal Engineering 2000 (pp. 1860-1870).

Chen, H., Zhang, J., Guo, Y., Cui, L., Guan, D., & Jiang, L. (2025). Laboratory modelling study on the scour characteristics around a jacket foundation subjected to combined wave-current loading. Renewable Energy, 122443.

Christiansen, N., Daewel, U., Djath, B., & Schrum, C. (2022). Emergence of large-scale hydrodynamic structures due to atmospheric offshore wind farm wakes. Frontiers in Marine Science, 64. https://doi.org/10.3389/fmars.2022.818501

CMEMS (2023a, 2023b). Atlantic - European North West Shelf - Ocean Physics Reanalysis. doi: 10.48670/moi-00059 and 10.48670/moi-00060

COWRIE (2010). A Further Review of Sediment Monitoring Data. Cowrie Ltd., Project reference ScourSed-09.

DECC (2008). Dynamics of scour pits and scour protection - Synthesis report and recommendations (Milestones 2 and 3), Department for Energy and Climate Change, Final Report.

Du, S., Wu, G., Zhu, D. Z., Wang, R., Lu, Y., & Liang, B. (2022). Experimental study of local scour around submerged square piles in combined waves and current. Ocean Engineering, 266, 113176.

Escarameia, M., and May, R. W. P. (1999). "Scour around structures in tidal flows.", HR Wallingford, Wallingford, U.K.

EGS (International) Ltd (2012). Lynn and Inner Dowsing Offshore Wind Farms, Year 3 Post-Construction Survey (2011), Phase 1 – Geophysical Survey (Job No. 4918, Final Report – Rev 7, CREL Reference No LD-O-EV-013-0000-000000-368-D). Marine data exchange. *https://www.marinedataexchange.co.uk/details/TCE-1041/2011-egs-lynn-and-inner-dowsing-year-3-post-construction-survey-phase-1---geophysical-survey/summary*

EGS (International) Ltd (2013). Lynn and Inner Dowsing Offshore Wind Farms (October 2012) (Job No. 5038, Final Report – Rev1). Marine data exchange. *https://www.marinedataexchange.co.uk/details/TCE-1076/2012-egs-lynn-and-inner-dowsing-offshore-wind-farms-post-construction-hydrographic-and-geophysical-survey/summary*

EU (2020). An EU Strategy to harness the potential of offshore renewable energy for a climate neutral future. European Commission, Communication COM/2020/741 final

Gabriel, K.R. (1971) The Biplot Graphic Display of Matrices with Application to Principal Component Analysis. Biometrika, 58, 453-467. http://dx.doi.org/10.1093/biomet/58.3.453

Gazi, A. H., Purkayastha, S., & Afzal, M. S. (2020). The equilibrium scour depth around a pier under the action of collinear waves and current. Journal of Marine Science and Engineering, 8(1), 36.

https://doi.org/10.5194/wes-2025-41
Preprint. Discussion started: 21 March 2025

Gușatu, L.F., Menegon, S., Depellegrin, D., Zuidema, C., Faaij, A., Yamu, C., 2021. Spatial and temporal analysis of cumulative environmental effects of offshore wind farms in the North Sea basin. Sci. Rep. 11, 1–18. https://doi.org/10.1038/s41598-021- 89537-1.

Harasti, A.; Gilja, G.; Adžaga, N.; Škreb, K.A. Principal Component Analysis in development of empirical scour formulae. In Proceedings of the 7th IAHR Europe Congress, Athens, Greece, 7–9 September 2022; pp. 271–272.

Harris, J. M., Herman, W. M. and Cooper, B. S. (2004). O_shore windfarms an approach to scour assessment, in Y. M. Chiew, S.-Y. Lim and N.-S. Cheng (eds), Proceedings of the 2nd nternational Conference on Scour and Erosion, Stallion Press, Singapore, pp. 283{291.

Harris, J. M., Tavouktsoglou, N. S., Couldrey, A., Whitehouse, R. J., & Klapper, J. (2023). Scour prediction in cohesive marine soils: a hybrid approach. *ISSMGE International Journal of Geoengineering Case Histories*, *7*(4), 59-75.

Hancu, S. (1971). Sur le calcul des a_ouillements locaux dans la zone des piles de ponts, Proceedings of the 14th IAHR Congress, pp. 299{313.

Hjorth, P. (1975). Studies on the nature of local scour. Bulletin Series A, Vol. 46, Department of Water Resources Engineering, Lund Institute of Technology, Schweden.

Kenyon, N. and Cooper, B. (2005). Sand banks, sand transport and o shore wind farms, Gov.British.

Laursen, E. M. (1963). An analysis of relief bridge scour, Journal of Hydraulics Division, Proceedings of the ASCE 89(HY3): 93{118.

Louwersheimer, W. F., Verhagen, H. J. and Olthof, J. (2009). Scour around an offshore windturbine, Coastal Structures 2007 - Proceedings of the 5th Coastal Structures Inter- national Conference, CST07, Venice, Italy, pp. 1903{1912.

London Array Ltd (2005). Environmental Statement Volume 1: O shore Works, Technical report, London Array Ltd.

Lyu, X., Cheng, Y., Wang, W., An, H., & Li, Y. (2021). Experimental study on local scour around submerged monopile under combined waves and current. Ocean Engineering, 240, 109929.

May, R. P. and Willoughby, I. R. (1990). Local scour around large obstructions, HR Wallingford Report SR240.

Matutano, C., Negro, V., López-Gutiérrez, J.-S. and Esteban, M. D. (2013). Scour prediction and scour protections in offshore wind farms, Renewable Energy 57: 358{365.

McGovern, D. J., Ilic, S., Folkard, A. M., McLelland, S. J., & Murphy, B. J. (2014). Time development of scour around a cylinder in simulated tidal currents. Journal of Hydraulic Engineering, 140(6), 04014014.

Melling, G. J. (2015). Hydrodynamic and geotechnical controls of scour around offshore monopiles. University of Southampton, Ocean and Earth Science, Doctoral Thesis, 250pp.

https://doi.org/10.5194/wes-2025-41
Preprint. Discussion started: 21 March 2025

819 Melville, B. (2008, November). The physics of local scour at bridge piers. In Fourth international conference on scour
820 and erosion (pp. 28-38).
821 Noormets, R., Ernstsen, V., Bartholoma, A., Flemming, B. and Hebbeln, D. (2003). Local
822 scour in a tidal environment: a case study from the Otzumer Balje tidal inlet, southern North Sea, Poster reproduced
823 in Appendix A of O_shore Center Danmark (2006).
824 Qi, W. G., & Gao, F. P. (2014). Physical modeling of local scour development around a large-diameter monopile in
825 combined waves and current. Coastal Engineering, 83, 72-81.
826 Qi, M., Li, J. & Chen, Q. 2016 Comparison of existing equations for local scour at bridge piers: parameter influence
827 and validation. Natural Hazards 82, 2089–2105.
828 Richardson, M. D., Valent, P., Briggs, K., Bradley, J. and Griffin, S. (2001). NRL mine burial experiments,
829 Proceedings of the 2nd Australian-American Joint Conference on the Technologies of Mines and Mine
830 Countermeasures, Sydney, Australia, pp. 1{23.
831 Rivier, A., Bennis, A. C., Pinon, G., Magar, V., & Gross, M. (2016). Parameterization of wind turbine impacts on
832 hydrodynamics and sediment transport. Ocean Dynamics, 66, 1285-1299.
833 Rudolph, D., Bos, K. J., Luijendijk, A. P., Rietema, K. and Out, J. M. M. (2004). Scour around offshore structures -
834 Analysis of field measurements, in Y. M. Chiew, S.-Y. Lim and N.-S. Cheng (eds), Proceedings of the 2nd
835 International Conference on Scour and erosion, Stallion Press, Singapore, pp. 400{407.
836 Saathoff, J. E., Goldau, N., Achmus, M., Schendel, A., Welzel, M., & Schlurmann, T. (2024). Influence of scour and
837 scour protection on the stiffness of monopile foundations in sand. Applied Ocean Research, 144, 103920.
838 Sarkar, A. (2014, February). Scour and flow around submerged structures. In Proceedings of the Institution of Civil
839 Engineers-Water Management (Vol. 167, No. 2, pp. 65-78). Thomas Telford Ltd.
840 Sarmiento, J., Guanche, R., Losada, I. J., Rosendo, E. M., Guindo, A., & de Guevara, J. L. (2024). Scour processes
841 around pile clusters of jacket foundations under steady currents. Ocean Engineering, 313, 119502.
842 Schendel, A. (2018). Wave-current-induced scouring processes and protection by widely graded material. Leibniz
843 University Hannover, Dissertation. DOI: https://doi.org/10.15488/4453
844
845 Schendel, A.; Welzel, M.; Schlurmann, T.; Hsu, T.-W. (2020). “Scour around a monopile induced by directionally
846 spread irregular waves in combination with oblique currents”. In: Coastal Engineering 161, 103751. DOI:
847 10.1016/j.coastaleng.2020.103751.
848 Schultze, L. K. P., Merckelbach, L. M., Horstmann, J., Raasch, S., & Carpenter, J. R. (2020). Increased mixing and
849 turbulence in the wake of offshore wind farm foundations. Journal of Geophysical Research: Oceans, 125(8),
850 e2019JC015858.
851 Sheppard, D. M., Odeh, M. and Glasser, T. (2004). Large Scale Clear-Water Local Pier Scour Experiments, Journal of
852 Hydraulic Engineering 130(10): 957{963.
853 Shields, M. A., Woolf, D. K., Grist, E. P., Kerr, S. A., Jackson, A. C., Harris, R. E., ... & Side, J. (2011). Marine
854 renewable energy: The ecological implications of altering the hydrodynamics of the marine environment.
855 Ocean & coastal management, 54(1), 2-9.
856 Soulsby, R. (1997). Dynamics of Marine Sands, Thomas Telford Ltd.

https://doi.org/10.5194/wes-2025-41
Preprint. Discussion started: 21 March 2025

Stahlmann, A. (2013, June). Numerical and experimental modeling of scour at foundation structures for offshore wind turbines. In ISOPE International Ocean and Polar

Sturt, F., Dix, J. K. and EMU Ltd (2009). The Outer Thames Estuary Regional Environmental Characterisation, Marine Aggregate Levy Sustainability Fund, 09/J/1/06/1305/0870, Technical report, Marine Aggregate Levy Sustainability Fund.

Sumer, B. M., Fredsoe, J. and Christiansen, N. (1992b). Scour around vertical pile in waves, Journal of Waterway, Port, Coastal and Ocean Engineering 118: 15.

Sumer, B. M., & Fredsøe, J. (2001). Scour around pile in combined waves and current. Journal of hydraulic engineering, 127(5), 403-411.

Teilmann, J., Carstensen, J., 2012. Negative long term effects on harbour porpoises from a large scale offshore wind farm in the Baltic - evidence of slow recovery. Environ. Res. Lett. 7 https://doi.org/10.1088/1748-9326/7/4/045101.

Van Rijn, L. C. (1984). Sediment transport, part I: bed load transport. Journal of hydraulic engineering, 110(10), 1431-1456.

Vanhellemont, Q., & Ruddick, K. (2014). Turbid wakes associated with offshore wind turbines observed with Landsat 8. Remote Sensing of Environment, 145, 105-115.

Walker, W. (1995). Field measurements of local pier scour in a tidal inlet, Msc, University of Florida.

Watson, S. C., Somerfield, P. J., Lemasson, A. J., Knights, A. M., Edwards-Jones, A., Nunes, J., ... & Beaumont, N. J. (2024). The global impact of offshore wind farms on ecosystem services. Ocean & Coastal Management, 249, 107023.

Welzel, M., Schendel, A., Schlurmann, T., & Hildebrandt, A. (2019). Volume-based assessment of erosion patterns around a hydrodynamic transparent offshore structure. Energies, 12(16), 3089.

Welzel, M. (2021). Wave-current-induced scouring processes around complex offshore structures.

Welzel, M., Schendel, A., Satari, R., Neuweiler, I., & Schlurmann, T. (2024). Spatio-temporal analysis of scour around complex offshore foundations under clear water and live bed conditions. Ocean Engineering, 298, 117042.

Wilson, J. C., & Elliott, M. (2009). The habitat-creation potential of offshore wind farms. Wind Energy: An International Journal for Progress and Applications in Wind Power Conversion Technology, 12(2), 203-212.

Whitehouse, R. J. S., Harris, J. M., Mundon, T. R. and Sutherland, J. (2010). Scour at Offshore Structures, Proceedings of the 5th International Conference on Scour and Erosion, San Francisco, pp. 11{20.

Whitehouse, R. J. S., Harris, J. M., Sutherland, J. and Rees, J. (2011). The nature of scour development and scour protection at onshore wind farm foundations. Marine Pollution Bulletin 62(1): 73(88).

Yao, Y., Chen, Y., Zhou, H., & Yang, H. (2016). Numerical modeling of current loads on a net cage considering fluid–structure interaction. Journal of Fluids and Structures, 62, 350-366.

Zhao, M., Zhu, X., Cheng, L., & Teng, B. (2012). Experimental study of local scour around subsea caissons in steady currents. Coastal Engineering, 60, 30-40.